Flinders UNIVERSITY

Title: Negative ion formation through dissociative electron attachment to the group IV tetrachlorides: Carbon tetrachloride, silicon tetrachloride and germanium tetrachloride

Authors: R. Kumar T P, B. Brynjarsson, B. Ómarsson, M. Hoshino, H. Tanaka, P. Limão-Vieira, D.B. Jones, M.J. Brunger, O. Ingólfsson

PII: S1387-3806(17)30403-7
DOI: https://doi.org/10.1016/j.ijms.2018.01.001
Reference: MASPEC 15913

To appear in: *International Journal of Mass Spectrometry*

Received date: 26-9-2017
Revised date: 28-12-2017
Accepted date: 1-1-2018

Please cite this article as: R.Kumar T P, B.Brynjarsson, B.Ómarsson, M.Hoshino, H.Tanaka, P.Limão-Vieira, D.B.Jones, M.J.Brunger, O.Ingólfsson, Negative ion formation through dissociative electron attachment to the group IV tetrachlorides: Carbon tetrachloride, silicon tetrachloride and germanium tetrachloride, International Journal of Mass Spectrometry https://doi.org/10.1016/j.ijms.2018.01.001

Negative ion formation through dissociative electron attachment to the group IV tetrachlorides: Carbon tetrachloride, silicon tetrachloride and germanium tetrachloride.

R. Kumar T P.[a], B. Brynjarsson [a], B. Ómarsson [a], M. Hoshino [b], H. Tanaka [b], P. Limão-Vieira [b,d], D. B. Jones[c],, M.J. Brunger [c] and O. Ingólfsson [a,*]
[a] Department of Chemistry and Science Institute, University of Iceland, 107 Reykjavík, Iceland
[b] Department of Physics, Sophia University, Tokyo 102-8554, Japan
[c]College of Science and Engineering, Flinders University, Adelaide, SA 5001, Australia
[d] Laboratório de Colisões Atómicas e Moleculares, CEFITEC, Departamento de Física, Faculdade de Ciências e Tecnologia, Universidade Nova de Lisboa, 2829-516 Caparica, Portugal

Graphical abstract

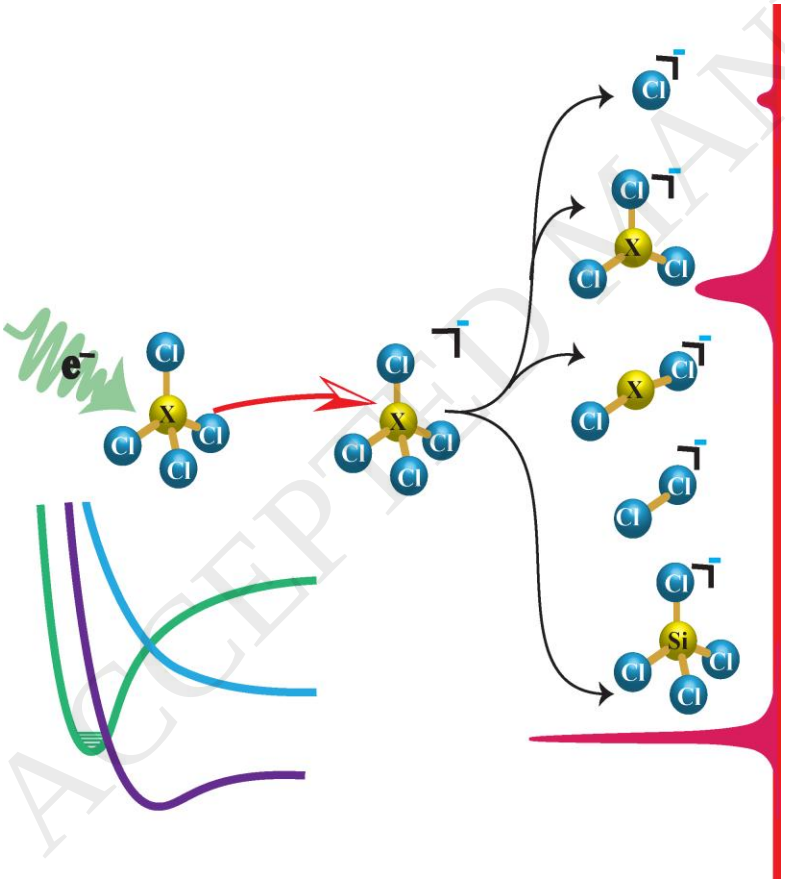

Highlights

- Dissociative electron attachment to the group IV tetrachlorides; XY_4 (X = C, Si, Ge).
- Literature review of electron scattering from the group IV tetrachlorides; XY_4 (X = C, Si, Ge).
- Last of three papers on dissociative electron attachment to the group IV tetrahalides; XY_4 (X = C, Si, Ge and Y = F, Cl, Br).

Abstract: The current contribution constitutes the third and final part of our trilogy of papers on electron attachment reactions of the group IV tetrahalides; XY_4 (X = C, Si, Ge and Y = F, Cl, Br). In this context we extend our previous studies on XF_4 and XBr_4 and report results for electron attachment to the tetrachlorides: CCl_4, $SiCl_4$ and $GeCl_4$ in the incident electron energy range from about 0 to 10 eV. At the same time we give a summary of the currently available literature on electron interactions with those latter compounds. Upon electron attachment the formation of Cl^-, XCl_3^-, XCl_2^- and Cl_2^- is observed from all the tetrachlorides, and additionally the molecular anion $SiCl_4^-$ is observed from $SiCl_4$. The main DEA contributions are observed through narrow, threshold peaks (at 0 eV) and we attribute these features to single particle resonances associated with the a_1 symmetry LUMOs of those compounds. Contributions from another low-lying resonance, which we assign as a $^2T_2$ shape resonance associated with the t_2 symmetry LUMO+1, is also observed in the ion yield curves for all the tetrachlorides. The energy of the peak position of those contributions varies in the range from about 1-2 eV, depending on the compound and the fragment formed. In addition to these low energy contributions, higher energy, fairly broad, features are observed for all the tetrachlorides. These contributions exhibit a peak in the energy range between 5 and 8 eV, again depending on the compound and the fragment formed. Further to the experimental data, we report DFT and coupled cluster calculations on the thermochemical thresholds for the individual fragments as well as the respective bond dissociation energies and electron affinities. These calculated values are compared with the experimental appearance energies and literature values, where they are available, with a quite fair level of correspondence being found.

1. Introduction

The current contribution is the third and last in our series of publications seeking to characterize negative ion formation from the group IV tetrahalides upon electron attachment. At the same time, we offer an overview of the literature on low energy electron interactions with those compounds. Note that our first contribution dealt with electron attachment to the tetrafluorides; CF_4, SiF_4 and GeF_4 [1], while the second study dealt with the tetrabromides; CBr_4, $SiBr_4$ and $GeBr_4$ [2]. In the current investigation, we report on our results for electron attachment to the tetrachlorides; CCl_4, $SiCl_4$ and $GeCl_4$ and we compare these results to those from earlier measurements, where possible.

Of the group IV tetrachlorides, CCl_4 is indisputably the most widely studied in the past. Its synthesis dates back to 1839 [3], and already by 1910 a patent was filed for its use as a fire extinguishing agent [4]. Its main utility has, however, been as a solvent, most noticeably in dry cleaning and also as a degreasing agent. Furthermore, it has been used extensively in the synthesis of refrigerants and propellants, and as a processing agent in numerous large-scale industrial processes [5]. In addition, CCl_4 has been used as a chlorine source in dry etching plasma processes [6]. Due to its ozone depletion potential, carbon tetrachloride was included in the Montreal Protocol in 1987 [7], and a prohibition on its use was agreed upon for developed countries by 1996 and by 2010 for article 5 countries (excluding an exemption for use as a processing agent). This was clearly an important step, as by 2008 CCl_4 amounted to about 11% of all tropospheric chlorine [8]. In the context of its atmospheric degradation and its use in plasma processing, a number of studies have examined how electrons interact with this species and the nature of its electronic structure. With respect to silicon tetrachloride, it is most noticeably used in the electronics industry for semiconductor manufacturing and plasma processes, as well as in the production of optical fibres and photovoltaic devices [9-13]. However, $SiCl_4$ is also an important intermediate in the production of polymeric silicone and other silicon based materials [14], [15]. Especially important is the use of $SiCl_4$ for the production of high purity silicon materials, where a high vapour pressure makes it suitable for silicon purification through fractional distillation [16]. Finally, we note that germanium tetrachloride is predominantly used in the production of GeO_2 containing glass in the core of fibre optics, where a high refractive index and low optical dispersion is essential [17]. It is also

employed in the production of other high purity germanium and germanium based materials [18], [19].

For the interpretation of dissociative electron attachment (DEA) and assignment of the underlying resonances, total cross sections (TCS) for electron scattering and electron transmission spectra, along with quantum mechanical calculations are an important aid. The TCSs are the sum of the integral cross sections for all energetically accessible processes, and enable the upper limit of scattering cross sections for the respective molecules to be established. In general, they exhibit a rather broad minimum with a rise at lower energies and one or more maxima below about 20 eV. The former is referred to as a "Ramsauer minimum" [20] and the latter are predominantly attributed to short-lived shape resonances, i.e. the formation of temporary negative-ions (TNIs). Further information on the TNIs is usually obtained through their decay processes, one of which is reemission of the electron via either elastic scattering or inelastic scattering involving vibrational and/or electronic excitation. Another is dissociation, i.e., DEA. For further insight into the formation and decay of negative ion resonances the reader is referred to the following review articles [21-24] and references therein. For polyatomic molecules, these resonances are often barely visible in the cross sections for elastic scattering and even for vibrational excitation due to overlapping of the resonant and non-resonant direct scattering contributions. However, where such resonances are antibonding -in the current cases for these with X-Cl σ* character- their formation leads to the excitation of the X-Cl symmetric stretching vibrations. Thus dissociation of the parent negative ion may occur on a comparable timescale as autodetachment, leading to the observation of a stable negative ion fragment.

For carbon tetrachloride the first TCS measurements for electron scattering were conducted by Holst and Holtsmark in 1931 [25]. In the 1980's and 1990's, further TCS measurements were reported by Szmytkowski *et al.* [26], covering the energy range from 0.5 to 200 eV, by Hamada and Sueoka [27] (0.7 to 400 eV), Jones *et al.* [28] (0.6 to 50 eV), Wan *et al*. [29] (0.2-12 eV) and Zecca *et al.* [30] (75 to 4000 eV). A review of all these data was given by Karwasz *et al* [31] in 2003, which also included the experimental determination of backward scattering from CCl_4 by Randell *et al*. [32] and theoretical work from Natalense *et al*. [33], [34] using the Schwinger Multichannel (SMC) method. Other theoretical work using the SMC method includes calculations of the elastic and rotationally inelastic cross sections by Varella *et al*. [35], and calculations of the integral and differential elastic cross sections by Azevedo *et al.* [36] and by

Moreira *et al*. [37]. Using a complex optical model potential formalism, Heng *et al.* [38], Shi *et al*. [39] and Gupta *et al*. [40] have also calculated the TCSs in the range from few tens of eV to 5000 eV. The first experimental measurements of the elastic differential cross section for CCl_4 were reported by Daimon *et al.* [41] in 1983, along with independent atom model calculations, for the energy range from 70 to 400 eV. More recently, Jiang *et al.* [42] have used combined *ab initio* pseudo-potential calculations to obtain elastic and inelastic cross sections and Curik *et al*. [43] have calculated the elastic integral and differential cross sections, up to about 20 eV, using close-coupled equations and a parameter-free model of the electron-CCl_4 interactions. However the only recent experimental electron scattering study we are aware of is the determination of the differential elastic scattering cross sections for CCl_4, in the range from 1.5 to 100 eV, conducted by Limão-Vieira *et al.* [44] in 2011. Further, these authors derived elastic integral and momentum transfer cross sections from their differential measurements.

Several studies of negative ion formation upon electron attachment to CCl_4 have been reported. The earliest of these dates back to 1938, where Baker and Tate [45] reported negative ion formation from the interaction of 75 eV electrons with CCl_4 vapour. In that study Cl^- formation was found to be the most efficient dissociation channel, followed by Cl_2^- formation whose intensity was about three orders of magnitude less. In addition the formation of C^- and CCl^- was also observed in that study [45], but with very low intensity. The Cl^- formation was attributed to dipolar dissociation (DD), however, it is not clear if those experiments were conducted under single collision conditions. Thus DEA due to low energy secondary electrons, or primary electrons that have lost the bulk of their energy through inelastic scattering processes, may have also contributed. In a later study by Reese *et al*. [46], DEA was found to lead to the formation of Cl^-, Cl_2^- and CCl_3^- with the Cl_2^- and CCl_3^- production being about two and three orders of magnitude less efficient than the Cl^- production, respectively. A further early study, concentrating on low energy Cl^- formation from CCl_4, was undertaken by Craggs *et al*. [47], where the author reported on Cl^- formation through DEA and DD covering the range from close to 0 eV up to about 70 eV.

In the meantime, the energy dependence of the Cl^- ion yield at low incident electron energies was studied in detail by a number of groups and a consistent picture for the formation of Cl^- from threshold (0 eV) up to about 2 eV emerged. Fox and Curran [48] reported the energy dependence of Cl^- formation from about 0-4 eV, Chu and Burrow [49] from about 0 to 2 eV,

Olthoff *et al*. [50] from about 0 to 3 eV and Hickam and Berg [51] reported the temperature dependency of Cl^- formation through DEA at incident energies below 4 eV. In this energy range the Cl^- ion yield is found to be characterized by two overlapping low energy peaks. The first, dominant, contribution is at threshold (0 eV) while the second is close to 0.8 eV. In the temperature dependence study by Hickam and Berg [51], the lower energy peak showed a distinct reduction in intensity when the gas temperature was increased from about 353 K to about 523 K. On the other hand, the higher energy peak was practically unaffected by the gas temperature. In another temperature dependence study by Spence and Schulz [52], however, a slight increase in the yield of the second peak was observed at higher temperature (1060 K). In two more recent low-energy studies by Matejcik *et al*. [53], [54], covering the temperature range from 300-550 K, the formation of Cl^- from CCl_4, at 0 eV and in the incident energy range around 0.8 eV, was not found to depend on the temperature. This is in agreement with swarm studies, which exhibited no temperature dependency of the rate constant for Cl^- formation from CCl_4 and thus confirmed the absence of an activation barrier for this reaction [55-58]. Matejcik *et al*. [53] point out that the previous observations may be influenced by thermal decomposition of CCl_4, leading to HCl formation and thus increased Cl^- formation at 0.8 eV [59]. The decrease in the 0 eV intensity with increasing temperature, on the other hand, is ascribed to the $T^{-0.5}$ temperature dependency of the number density of the molecular beam. In their studies, Matejcik *et al*. [53] also determined the relative cross section for Cl^- formation below 1 eV, with an electron energy resolution of 11 meV, and found that the energy dependence of the cross section for Cl^- from CCl_4 approaches the $2\pi\lambda$ limit at few 10s of meV incident electron energy (λ is the de Broglie wavelength of the electron), showing the E^{-1} dependence predicted for the s-wave de Broglie cross-section [60]. These results are in good agreement with an earlier higher resolution (6 meV) study by Chutjian and Alajajian [61], using the threshold photoionization technique, and covering the electron energy range from about 0 eV to 140 meV. More recently the threshold behaviour of Cl^- formation was further confirmed by Klar *et al*. [62], in an extensive laser photoelectron attachment experiment covering the electron energy range from about 0.8 meV, up to 173 meV with an electron energy resolution better than 1 meV. For a non-polar molecule, i.e., without permanent dipole, the polarizability governs the long-range interaction. In this case, which applies to CCl_4, the Vogt-Wannier model predicts the s-wave attachment cross section at very low energies, ($E \rightarrow 0$) to be proportional to $E^{-1/2}$ [63]. This describes the low energy limit of

the semi-empirical formula later proposed by Klots [64]. In their high-resolution study, extending down to below 1 meV, Klar et al. [62] use a variation of the Klots formula, to fit the experimentally determined cross section. With this approach an excellent description of the energy dependence of the attachment cross section is attained for the whole energy range from about 0.8 to about 50 meV, i.e., up to the threshold for the first vibrational excitation at about 57 meV. The cross section in this energy range varies from about 5.5×10^{-17} m^2 to about 10^{-18} m^2. The low energy limit described by the $E^{-1/2}$ proportionality, however, is only approached below 0.3 meV [62], which is outside the experimentally determined range in this study. For the exact functional forms used to reproduce the threshold behaviour of electron attachment to CCl_4, the reader is referred to the original literature cited here above and Klar et al. [62]. For a critical account on available experimental data on electron attachment to CCl_4 in the low energy/threshold region the reader is also referred to Klar et al. [62], which offers a comprehensive discussion on the threshold behaviour in electron attachment, models used to describe this and their agreement with experimental data.

Furthermore, by using an extended laser photoelectron attachment approach, with post acceleration of the photoelectrons, Hotop and co-workers [65] determined the absolute cross sections for Cl^- formation in the low energy range and for Cl_2^- up to an incident electron energy of 2 eV. That work was conducted with an electron energy resolution of about 20 meV.

In addition to these crossed-beam and photoelectron experiments, the low energy (thermal) electron attachment rate constants, for electron attachment to CCl_4, have been measured in a number of swarm studies using different techniques [55-58, 66-71]. These include the flowing afterglow/Langmuir probe (FALP) technique [69], the use of a discharge flow system coupled to an electron paramagnetic resonance (EPR) spectrometer and a quadrupole mass spectrometer [70], a pulse sampling technique [71] and a pulse-radiolysis microwave-cavity technique [56]. For the low energy region the electron attachment studies agree well, revealing a fast and barrier-less formation of Cl^- and with rate constants/cross-sections close to the s-wave attachment limit at very low electron energies.

From electron transmission spectroscopy (ETS) and Xα calculations ([49, 50, 72-74]) the first contribution, i.e., the threshold contribution, may be assigned to the formation of the $^2A_1$ ground state anion, which lies just below the neutral ground state. The 0.8 eV contribution, on the other hand, is attributed to the triply degenerate $^2T_2$ first excited state (LUMO+1) appearing at 0.94 eV

in the ETS [74] work. Further, it is worth noting from the very recent study by Li *et al*. [75] that they used the high intensity 0 eV Cl^- channel to demonstrate the feasibility of studying neutral radical formation in DEA, i.e., CCl_3 in this case.

Dissociative electron attachment studies on the energy dependence and the branching ratios for the formation of fragments other than Cl^-, at higher incident electron energies, are less abundant. To the best of our knowledge, these are confined to an investigation by Dorman *et al*. [76], conducted in the mid 1960's, and three investigations reported by the Illenberger group in Berlin in the 1980´s [77-79]. Those studies agree well with one another and report, in addition to Cl^-, the formation of Cl_2^-, CCl_2^- and CCl_3^-. From these anions, Cl_2^- and CCl_3^- are predominantly formed slightly above 1 eV, while CCl_2^- is predominantly formed close to 6 eV. Here the contributions close to 1 eV largely coincide with the $^2T_2$ resonance observed in the ETS at 0.94 eV, however, a resonance coinciding with the 6 eV DEA contributions is not observed in the ETS. Nevertheless, the TCS measurements for CCl_4 show a clear structure at about 7.5 eV, emerging from a broad contribution stretching to higher energies [27, 28, 80]. That structure is assigned to an E-symmetry shape resonance which is found to be located close to 9 eV in the partial cross section calculations by Curik *et al*. [43], and at about 8 eV in the Schwinger multichannel calculations by Moreira *et al*. [32] (at the static exchange approximation level). Due to competition with autodetachment, DEA ion yields are commonly shifted to lower energies, with regards to the respective resonance energies. This is especially true for high-energy open channel resonances where the autodetachment rate may be very significant. The 6 eV contributions in the DEA spectra for CCl_4 may thus correlate with the TCS structure at about 7.5 eV. We however note, that a shift of the ion yield towards lower energies with respect to the Franc-Condon overlap, is not general. Where the thermochemical threshold for the formation of the observed negative ion fragments is at higher energy or close to that of the onset of the respective resonance, a shift towards higher energies may be observed in the ion yield curves. This in turn, may explain the slight shift of the Cl_2^- and CCl_3^- low energy ion yield maxima as compared to the transition energy of the $^2T_2$ resonance as observed in ETS.

For silicon tetrachloride, we are only aware of two studies reporting the TCSs. The first was conducted in 1990 by Wan *et al.* [80], in the energy range from 0.2–12 eV, and the second in 1999 by Mozejko *et al*. [81], reporting results from two different apparatus configurations in the energy range from 0.3 to 4000 eV. In addition to these mainly experimental studies, Tossell and

Davenport [73] and Modelli *et al.* [74] used the continuum *MS-Xα* method to calculate elastic and total electron scattering cross sections, respectively. Both these investigations covered the incident electron energy range up to about 6 eV. Furthermore, Natalense *et al.* [33] employed a combined pseudo-potential, ab-initio technique to compute the integral elastic cross sections in the energy range from 0-40 eV, and Varella *et al.* [35] calculated the integral and differential elastic cross sections, as well as the rotationally inelastic cross-section, using the SMC method in the energy range between 0 to 30 eV. Elastic integral and differential scattering cross sections in the energy range from 20 to 2000 eV have also been calculated by Mozejko *et al.* [82], using the independent atom method (IAM) with a static-polarization model potential. More recently, Bettega *et al*. [83] extended their SMC calculations to compute elastic integral, differential and momentum transfer cross sections that cover the energy range from about 0 to 10 eV and the full 180° scattered electron angular range. Finally, Verma *et al*. [84] calculated total inelastic and ionization cross sections for silicon tetrachloride in the energy range from the ionization threshold up to 5000 eV, using a spherical complex optical potential formalism for the total inelastic cross sections.

Dissociative electron attachment studies on $SiCl_4$ are more numerous than these just described above for the experimental scattering investigations, but most of them are incomplete with regards to the energy dependence of the branching ratios for the individual fragments formed. The first DEA study on $SiCl_4$ was reported in 1947 by Vought *et al.* [85]. In that study the ion yield for Cl^- and $SiCl_2^-$ was reported over the energy range from about 0 to 10 eV (but note their energy scale was not calibrated). Both fragments were observed at low energies, with Cl^- apparently formed through two distinct resonances in the low energy region. Additionally, Cl^- was observed at a higher energy, i.e., at about 10 eV, in the uncalibrated spectra. Dorman *et al.* [76], on the other hand, reported the formation of both Cl^- and Cl_2^- in this energy range, with the Cl^- contribution rising exponentially towards 0 eV without any apparent second contribution at these low energies. However, those authors found that both Cl^- and Cl_2^- exhibited a high-energy contribution peaking at around 7 eV, which for Cl^- agrees at least qualitatively with the data from Vought *et al*. [85]. In addition to these fragments, Wilkerson and Dillard [86] observed the formation of the molecular anion $SiCl_4^-$ and the fragments $SiCl_3^-$, $SiCl_2^-$, $SiCl^-$, Si^- and Cl^-, using an ionization source from a mass spectrometer tuned to low acceleration energies (not specified) and at an incident electron impact energy of 50 eV. These experiments were carried

out at fairly high pressures, so that low-energy secondary electrons and electrons that have lost considerable energy through inelastic scattering processes are also likely to play a significant role. At low pressures (< 10^{-5} Torr), Wang *et al*. [87] observed the formation of the molecular anion $SiCl_4^-$ with a peak maximum at 0.5 eV, and Cl^- with peak maxima at 1.8 and 7.8 eV. The fragment $SiCl_2^-$ was also observed in this experiment, but only at elevated pressure. In a later study by the same group, Papst *et al.* [88] observed the formation of Cl^-, Cl_2^-, $SiCl_2^-$ and $SiCl_3^-$, through broad contributions with maxima in the range from about 7 to 9 eV, and an additional Cl^- contribution between 0 and 3 eV. Except for the Cl^- formation, however, this study only covered the energy range from about 4 to 12 eV, and thus does not shed any light on the low energy processes of the other anionic fragment formations. In a low pressure study by Moylan *et al.* [89], Cl^- was again found to be the dominant fragment. In that study, it was produced through a fairly narrow contribution at about 2 eV and a broader contribution peaking close to 10 eV. In addition, the fragments Cl_2^-, $SiCl_2^-$ and $SiCl_3^-$, as well as the molecular anion $SiCl_4^-$ and the secondary product $SiCl_5^-$, were observed. Importantly, however, those authors [89] stated: "*Like earlier workers, we observed dramatically different product distributions under different conditions, with no clear trend as to which parameters affected which products.*". The only other fairly complete study on DEA to $SiCl_4$ is that of Jäger and Henglein [90]. They reported the observation of Cl^-, Cl_2^-, $SiCl_2^-$ and $SiCl_3^-$, as well as the molecular anion $SiCl_4^-$. The molecular anion is by far the dominant anion formed in that work, but all other fragments are also observed at 0 eV incident electron energy and through a contribution peaking between about 6 to 7 eV. Additionally, a peak in the Cl^- contribution is observed at about 1.4 eV and in the $SiCl_3^-$ ion yield close to 1.7 eV. These experiments were, however, conducted at an elevated pressure of 10 Torr, and are thus not representative for DEA to $SiCl_4$ under single collision conditions. It is thus fair to say that the current data on negative ion formation from $SiCl_4$ upon electron attachment is incomplete, contradictory, and does not allow for a consistent interpretation of the relevant processes.

For germanium tetrachloride the only experimental electron scattering work known to us is the TCS measurement reported by Szmytkowski *et al.* in 1997 [91], for the energy range from 0.6 to 250 eV. Theoretical calculations on electron scattering from $GeCl_4$ are also limited in number. To our knowledge they are confined to the Xα TCS calculations by Guillot *et al.* [92] and Modelli *et al* [74], in the energy range from 0-6 eV, and calculations of the elastic integral and

differential scattering cross sections by Azevedo *et al.* [36] (0 to 30 eV), Joucoski and Bettega [93] (5-40 eV) and by Mozejko *et al.* [82] (20 to 2000 eV) as well as the total inelastic and ionization cross sections recently reported by Verma *et al*. [84] for the range from the ionization threshold to 5000 eV. The first two studies of the elastic cross sections employ the Schwinger Multichannel method, the third uses the independent atom model with a static-polarization model potential, while as noted previously the total inelastic cross sections reported by Verma *et al*. [84] are computed using a spherical complex optical potential formalism. In addition to the elastic integral and differential scattering cross sections, Azevedo *et al.* [36] also reported elastic momentum transfer cross sections in the energy range from about 4-30 eV.

Dissociative electron attachment studies on $GeCl_4$ are also limited in number. The first studies were reported by Pabst *et al*. [88] and by Mathur *et al.* [94] in 1977 and 1979, respectively. The former [88] reports the formation of Cl^-, $GeCl_2^-$ $GeCl_3^-$ and Cl_2^- anions. All these fragments were observed through a broad contribution peaking at around 6 eV, while $GeCl_3^-$ is also observed through a narrower contribution peaking at about 2 eV. The later of these studies [94] reports on the formation of $GeCl_3^-$ in the collisions of $GeCl_4$ with Cs,, with the energetics for $GeCl_3^-$ formation and the electron affinity of $GeCl_3$ being discussed briefly. In addition to those original investigations we are also aware of two combined DEA/ETS studies. Guillot *et al.* [92] carried out a detailed electron transmission and dissociative electron attachment study, along with X-ray absorption spectroscopy (XAS), inner shell electron energy loss spectroscopy (ISEELS) and *ab initio* calculations. The ETS of $GeCl_4$ shows two resonances, the first is found to be of t_2-symmetry and is located at 1.72 eV while the second, weaker, one is of *e*-symmetry and is located at 5.6 eV. In their DEA study, Guillot *et al.* [92] detected three fragment anions: Cl^-, $GeCl_2^-$ and $GeCl_3^-$, each with a single peak at 0.0, 5.5 and 5.7 eV, respectively. A later study by the same group (Modelli *et al.* [74]) confirmed those results. Although the energy dependence of the DEA fragment formation from $GeCl_4$, reported by Guillot *et al.* [92] and Modelli *et al.* [74], is well substantiated, the lack of any ion contribution through the 1.72 eV t_2-symmetry resonance observed in their ETS is surprising. This is especially true when taken in context with CCl_4 and $SiCl_4$, where the corresponding t_2-symmetry resonance apparently contributes markedly to the ion yield. Furthermore, the low intensity of their $GeCl_2^-$ signal and the lack of any Cl_2^- ion yield is not in agreement with the earlier observations by Pabst *et al*. [88], where both these fragments were observed with appreciable intensity.

In the current contribution we report on measurements of electron attachment to the three group IV tetrahalides, in the energy range from 0 to about 10 eV. Appearance energies for each of the fragments formed are reported and compared with calculations of the respective thermochemical thresholds. Calculated electron affinities (EAs) for Cl, Cl_2, XCl, XCl_2 XCl_3 and XCl_4 and the bond dissociation energies (BDEs) for the sequential loss of the halogens are also presented. These values are compared with experimental values from the literature, where they are available. For CCl_4 our data agrees well with previous measurements, and further substantiates the current understanding of DEA to this compound as was outlined above. For $SiCl_4$ where, despite the number of available DEA studies, no consistent picture of those processes has emerged, we are able to provide reliable data and a consistent interpretation of the energy dependence of the anion formation upon electron attachment to this compound. Furthermore, we can also, at least partly, offer an explanation for the inconsistency of the previous data. Finally, for $GeCl_4$ our data offers a complete picture of the anion formation upon electron attachment to this compound and clarifies the discrepancies between the earlier studies.

The structure of the remainder of this paper is as follows. In Section 2 we provide details of our experiments and calculations, and any analysis tools we implement in order to assist us in the interpretation of the data. Thereafter, in Section 3, we provide our results and a discussion of those results for each individual compound. Finally, some conclusions are drawn in section 4.

2. Methods

2.1. Experimental

All the present measurements were conducted using a crossed electron-molecule beam apparatus under single collision conditions. The instrumental configuration has been described in detail previously [95] and we thus only give a brief description here. A quasi-monochromatic electron beam is generated using a trochoidal electron monochromator (TEM) and crossed with an effusive beam of the molecules under investigation. For $GeCl_4$ and $SiCl_4$ the electron energy scale was calibrated based on the measurement of SF_6^- formation from SF_6, and O^- formation from CO_2. The peak position for SF_6^-/SF_6 is at 0 eV and the peak positions for O^- from CO_2 are at 4.4 and 8.2 eV, respectively [96]. For CCl_4 both the Cl^- formation from CCl_4 at 0 eV, and O^- formation from CO_2, were used to calibrate the electron energy scale. The energy resolution of the electron beam was estimated from the full width at half maximum (FWHM) of the 0 eV SF_6^-

signal from SF_6 and of the Cl^- signal from CCl_4. The so measured resolution was in the range from 110 to 130 meV during the current measurements.

Negative ions produced in the reaction chamber were extracted with a weak electric field (< 1 V/cm) and analysed and detected with a quadrupole mass spectrometer (Hiden EPIC1000). Ion yields were recorded with the quadrupole mass filter set to allow only transmission of one mass and by scanning the electron energy. The background pressure prior to the experiments was ~$6x10^{-8}$ mbar and the experiments were conducted in the working pressure range from $5x10^{-7}$ to $2x10^{-6}$ mbar. The only exception to that is for the Cl^-/CCl_4 measurement, where we used a working pressure of ~$8x10^{-8}$ mbar. All experimental measurements were carried out with the gas inlet system at room temperature, however, to avoid condensation of residual molecules on the electron lens components the monochromator was maintained at ~393 K. The compound $GeCl_4$ was purchased from Sigma Aldrich with a stated purity of 99.99%, $SiCl_4$ was purchased from Strem Chemicals with a stated purity of 99.9999% and the compound CCl_4 was purchased from Merck with a stated purity of >99%. $SiCl_4$ and $GeCl_4$ were used without further purification, while CCl_4 was distilled over P_2O_5 prior to use. While CCl_4 is stable at ambient conditions, $SiCl_4$ and $GeCl_4$ readily hydrolyse in contact with air. To avoid any hydrolysis, as far as this is possible, these samples were pre-loaded into a sample vessel terminated with a ball valve in a nitrogen filled glove box. The valve was then attached to the inlet system, below a second ball valve, and the void between both valves was pumped out through the vacuum chamber, before opening the valve sealing the sample vessel. The molecular flow into the reaction chamber was controlled using a precision leak valve (MDC vacuum products). Finally, note that special care was taken to bake out the inlet system prior to attaching the sample holder.

2.2. Appearance energies

The appearance energies of the negative ion fragments observed in DEA are not directly related to the corresponding threshold energies for the respective fragment formation. Rather, they describe the low energy region of the respective resonances, where the transition probability within the Frank-Condon region becomes non-zero and the lifetime of the temporary negative ion formed is sufficient for dissociation to occur [97]. A direct relation to the respective threshold energies is thus only to be expected when these are higher than the onset of the respective resonances. Furthermore, the current experiments were conducted at room temperature and thereby constitute a Maxwell-Boltzmann distribution of internal energies with a most probable value of about 180 meV. This internal energy, along with the finite energy resolution of the electron beam (110 - 130 meV), may cause the measured AEs to be below the actual threshold energy values, even if they are above the energy threshold of the respective resonances.

In our previous contributions on the group IV tetrafluorides and tetrabromides [1, 2], the appearance energies for the anions observed were determined by fitting the onset of the ion yield curves with a Wannier type function [98] of the form:

$$f(E) = b + c(E - AE)^p. \qquad (1)$$

Here E is the incident electron energy, b is a constant to account for any background signal, c is a scaling factor, AE is the appearance energy of interest and p is the Wannier exponent. To account for the energy resolution of the incident electron beam, this threshold function was convoluted with a Gaussian function with the same FWHM as the energy resolution of the electron beam during the respective measurements. The internal energy distribution was not explicitly taken into account here.

For the sake of self consistency, we adhere to this approach for the determination of the AEs of the negative ion fragments from the group IV tetrachlorides reported in this study. This is, however, as stated previously [1, 2], a functional form that does not bear physical meaning to the DEA process. In fact, this functional form was derived to describe the electron impact ionization of atomic targets [99], but has since become commonly used to determine ionization energies and AEs in dissociative ionization of molecular targets [100-102].

For comparison we have also determined the appearance energies through linear fits to the respective ion yield curves, as we did in our contribution on the group IV tetrabromides [2].

Here, however, we take the baseline-interception of a linear fit to the ion yield onset region as the AE lower limit, and a linear fit to the rising edge of the peak as the AE upper limit, with the stated AEs being the average of these two values (see S1). This approach is bound to be somewhat subjective and for transparency, representative examples of such linear fits, and of the fits using equation 1, are shown for all fragments as supporting material (Figure SI 1). Note that results from the two approximations are largely consistent within their combined uncertainties.

Only linear fits were used to determine the AEs for overlapping peaks and where the signal intensity and/or signal to noise ratio was very low. This is indicated in the respective tables. Only one data set is behind the AEs determined for $GeCl_3^-$ and CCl_3^-. For Cl_2^- from $GeCl_4$ and for $SiCl_2^-$ and the high-energy contribution from $SiCl_3^-$ two data sets are behind the reported AEs. All other fits were performed on three independent data sets. The error margins are estimated from the standard deviation of the mean of the AEs derived from these data sets. For $GeCl_3^-$ and the high energy CCl_3^- contribution the reported error margins are those from the uncertainty determined from the fitting of the respective ion yield curves. In some cases, the uncertainty determined is < 0.1 eV. Where this is the case, we report a lower limit uncertainty of 0.1 eV in the derived AEs. Please note that a low signal to noise ratio contributes significantly to the determined uncertainty, and therefore the quoted error margins are higher when the ion yield signal is low. Finally, where impurity signals overlap with the onset of the ion signals the AEs are simply estimated from a linear fit to the rising edge of the respective signals.

2.3. Calculations

All threshold energy calculations were performed using the ORCA computational chemistry software [103]. The total energy of the parent molecules and relevant neutral and charged fragments were calculated using both DFT (B2PLYP) [104] and coupled cluster (CCSD(T)) [105] methods. The functional B2PLYP was originally selected for our previous study on the group IV tetrabromides based on the performance of B2PLYP in a thorough benchmarking study with number of functionals for the calculation of thermochemical properties of compounds composed of main group elements [106]. We found that this functional performed well in predicting the thermochemical thresholds for negative ion formation through DEA to $GeBr_4$, $SiBr_4$ and CBr_4 except for the very low intense contribution of CBr_2^-/CBr_4 and $SiBr_3^-/SiBr_4$. For consistency, we used the same functional here, however, as we found that this functional apparently overestimated some of the threshold values we additionally used a coupled cluster

(CCSD(T)) approach for comparison (see discussion in the results and discussion section). The 6-31G basis set [107] was used for B2PLYP calculation, while an extrapolation of aug-cc-pVTZ and aug-cc-pVQZ [108] was used for the CCSD(T) calculation. The zero-point energy (ZPE) contributions were calculated for all multi-atom fragments and included in the total energy. Thermochemical thresholds for all the negative ion fragments were calculated by subtracting the ground state minimum energy of the negative ion and neutral fragments from the minimum energy of the ground state parent molecule. The electron affinities (EAs) of the fragments were calculated by subtracting the total energy of the ground state neutral fragment from that of the respective anionic fragments. Bond dissociation energies were then derived by subtracting the electron affinity of the fragment formed from the threshold energy for the relevant process.

3. Results and discussions

The group IV tetrachlorides, XCl_4 (X = C, Si and Ge) all have tetrahedral symmetry with X as the central atom and thus belong to the t_d symmetry group. Optimized bond angles between adjacent X−Cl bonds are that of a tetrahedron; namely 109.47°. The optimized bond lengths between the central atom and the Cl atoms in CCl_4 is 1.762 Å; in $SiCl_4$ it is 2.018 Å and in $GeCl_4$ it is 2.117 Å [109]. In order of increasing energy the occupied valence orbitals of XCl_4 are expected to be; ...a_1^2, t_2^6, a_1^2, t_2^6, e^4, t_2^6, t_1^6 [110]. From these the two lowest-lying orbitals; a_1 and t_2 are bonding X−Cl σ orbitals, while the remaining are non-bonding orbitals with mainly halogen lone-pair character [110]. The first two unoccupied virtual molecular orbitals of XCl_4 are both anti-bonding X−Cl σ* orbitals. The first of these, the LUMO, is of a_1 symmetry while the LUMO+1 is a triply degenerate molecular orbital of t_2 symmetry. Correspondingly, $^2A_1$ and $^2T_2$ single particle negative ion resonances associated with the low-lying a_1 and t_2 molecular orbitals may be expected. Similarly two-particle-one-hole resonances of T_1 and T_2 symmetry, formed through electron excitation from the bonding t_1 HOMO and t_2 HOMO−1 to either the a_1 LUMO or the t_2 LUMO+1 might also be anticipated.

3.1 Carbon tetrachloride

Figure 1 shows the energy dependence of the negative ion yield for all ion fragments observed upon electron attachment to CCl_4 in the energy range from about 0 to 10 eV. The vertical arrows indicate the appearance energy of each anion, determined from the Wannier type fits as outlined in section 2.2. In addition, dotted-line arrows show the thermochemical thresholds of each anion as calculated at the CCSD(T) level of theory.

From Figure 1 it is apparent that electron attachment to CCl_4, in the energy range from 0 to 10 eV, leads to the formation of Cl^-, Cl_2^-, CCl_2^- and CCl_3^-. The molecular anion CCl_4^- is not detected, which is in accordance with the short life-time of the TNI formed upon electron attachment. Kalamarides *et al*. [111] determined the lifetime of the CCl_4^- TNI formed, through electron transfer in collisions of CCl_4 with *K(nd)* Rydberg atoms, and found it to be about 30 ps. In our experiment, the extraction field in the ionization region does not exceed 1 V/cm, resulting in an extraction time of about 10 μs and the flight time through the quadrupole mass filter is on the order of 50 μs. Hence, the lifetime of the CCl_4^- TNI is considerably shorter than our window of observation.

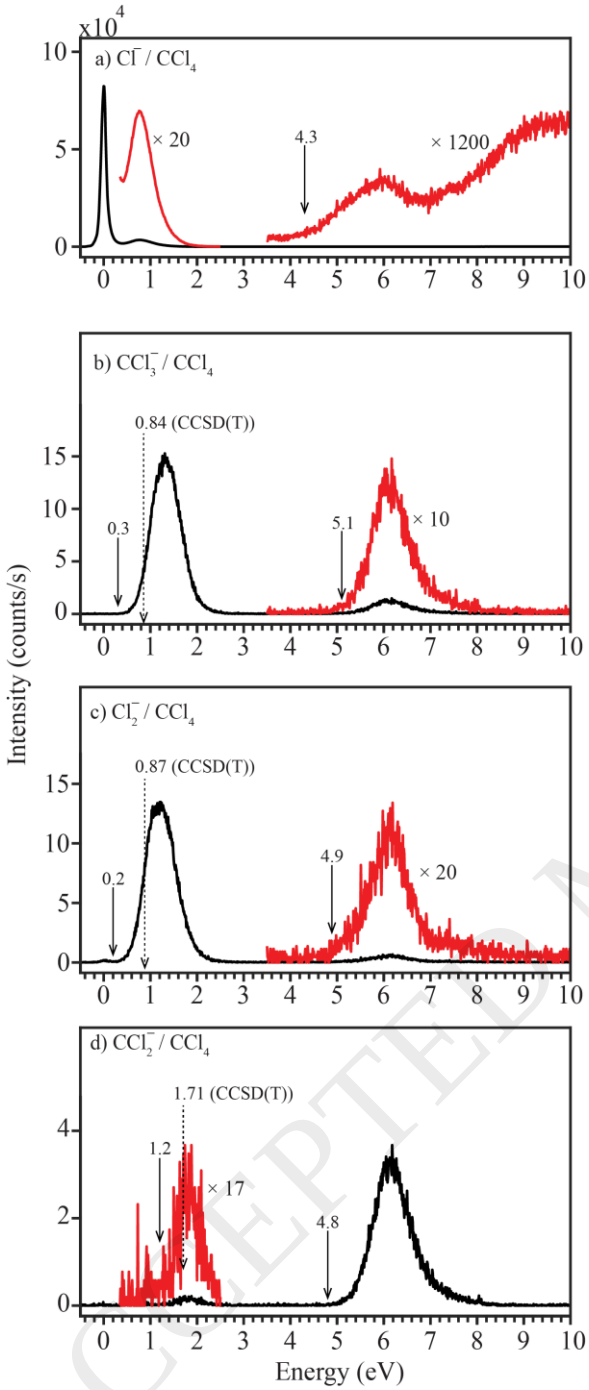

Figure 1. Dissociative electron attachment ion yield curves for CCl_4 in the energy range from ~0 to 10 eV. The solid-line arrows indicate the appearance energy (eV) determined from the fitting to the rising part of the ion yield curves using a Wannier type function except for the Cl^- negative ion yield curve where the appearance energy is determined from the linear fits (see Section 2.2). Dotted-line arrows show the threshold energy (eV); E_{th}, calculated at the CCSD(T) level of theory. Intensity shown on the y axis is normalized with respect to the pressure.

In good agreement with previous experiments we find that the most efficient channel is the formation of Cl^- at threshold. This channel is characterized by a narrow-width peak at 0 eV

incident electron energy. A second contribution is also observed in the Cl^- ion yield peaking at about 0.8 eV with an intensity that is in the current experiment about $1/20^{th}$ of that observed for the 0 eV peak. The positions of these low-energy features in the ion yield for Cl^- agree well with previous studies [48, 50, 51, 53, 77, 79]. Their relative intensities are also in qualitative accord with what has been reported previously, in experiments with similar energy resolution and detection systems. However in general these intensities cannot be compared directly between different experiments, especially when the electron energy resolutions and extraction optics differ. The absolute cross section for the Cl^- formation in the low energy region has, however, been determined in previous studies [53, 65], and is found to be about 5×10^{-20} m^2 for the second contribution at 0.8 eV. At about 10 meV impact energy the cross section is about 1×10^{-17} m^2 [62], and it approaches the $\pi\lambda^2 \propto E^{-1}$ limit for s-wave attachment [112] at very low incident energy. An excellent fit to this data was achieved by Klar *et al.* [62] with a modified form of the Klots formula [64] converging towards the $E^{-1/2}$ dependence at very low energies (below 0.3 meV), as is discussed in the introduction here above. For a comprehensive discussion on the energy dependence and absolute cross sections for Cl^- formation from CCl_4, at energies below about 1 eV, the reader is referred to reference [62] and references therein.

From Xα calculations, the $^2A_1$ anionic ground state of CCl_4^- is expected to lie about 0.5 eV below threshold, and the triply degenerate $^2T_2$ resonance is expected to be at about 0.94 eV [74]. This is in good agreement with ETS studies [49, 50, 72], where only one clear transition is observed for CCl_4 at 0.94 eV and is assigned to that $^2T_2$ shape resonance. The $^2A_1$ resonance, on the other hand, is not observable in ETS as it is energetically below threshold. Both swarm [55, 66, 68], and high-resolution photoelectron and beam studies [62, 65], however, show very high rate coefficients/cross sections for the Cl^- formation at threshold. Correspondingly, the 0 eV contribution in the Cl^- negative ion yield is attributed to the $^2A_1$ resonance while the contribution at around 0.8 eV is assigned to the $^2T_2$ resonance associated with a single electron occupation of the t_2 symmetry LUMO+1.

Further contributions to the Cl^- yield are observed at higher energies, through a peak maximum at around 6 eV, followed by a continuous contribution above that energy. This contribution gradually increases with an increasing incident electron energy before levelling off. In this energy range the total scattering cross sections exhibit a broad peak with a maximum at around 7.5 eV, and a significant shoulder towards higher energies [26-28]. Furthermore, calculations by

Tossell and Davenport [73] and more recently by Curik *et al*. [43], locate a broad E-symmetry resonance at about 9 eV. Note that this feature is found at about 8 eV in the Schwinger multichannel calculations performed at the static-exchange approximation level by Moreira *et al*. [32].

Generally, high-energy shape resonances may appear in the DEA ion yield with a significant shift towards lower energy due to the competition between autodetachment and dissociation mechanisms [97]. Therefore, from the electron scattering TCS result of CCl_4, it may be appropriate to assign the high-energy resonance feature centred at about 6 eV in the Cl^- yield to an E symmetry shape resonance apparent at about 7.5 eV in the total scattering cross sections. However, we note that core excited resonances cannot be excluded at this impact energy. Finally, the non-resonant high-energy contribution, above 6 eV in the Cl^- ion yield, is attributed to dipolar dissociation.

In addition to Cl^-, we observe the formation of Cl_2^-, CCl_3^- and CCl_2^- through DEA in the energy range from 0 to about 10 eV (see Figure 1). In Table 1 the appearance energies and the peak maxima for the individual negative ion contributions are listed, along with the results from the current CCSD(T) and B2PLYP DFT calculations of the thermochemical thresholds for the formation of the respective ions. For comparison, appearance energies and peak intensity energy values reported in the earlier, energy calibrated, study by Scheunemann *et al*. [77] are also listed along with the peak values we estimated from the ion yield curves reported by Oster et al. [78].

The ion yield curves for the fragments Cl_2^-, CCl_3^- and CCl_2^- (shown in Figure 1.) are all similar, with a low energy contribution peaking at 1.2, 1.3 and 1.8 eV, respectively. We attribute these contributions to the triply degenerate $^2T_2$ resonance observed at about 0.94 eV in the ETS [74]. The shift towards higher energy, as compared to the Cl^- formation at 0.8 eV, and along the lines $AE(Cl_2^-) < AE(CCl_3^-) < AE(CCl_2^-)$, is attributed to the progressively higher thermochemical thresholds for the respective processes. We have calculated the threshold energies for these processes at the B2PLYP and CCSD(T) level of theory, assuming that the neutral counterpart to Cl_2^-, i.e., CCl_2, stays intact. For CCl_2^- the threshold is calculated both under the assumption that this fragment is formed through the loss of Cl_2 and through the loss of two Cl atoms (see Table 1). Compared to the experimental AEs determined using a Wannier fit to the ion onset region, the thermochemical thresholds calculated at the CCSD(T) level of theory

are in all three cases about 0.5 - 0.6 eV above the experimental appearance energies. The thermochemical thresholds calculated at the B2PLYP DFT level of theory are somewhat lower in value than those calculated at the CCSD(T) level of theory, but are in all three cases still about 0.4 eV above the experimental appearance energies. Despite the fact that the available thermal energy at room temperature (about 180 meV) is not accounted for in the 0 K thermochemical threshold values reported, and that allowance should be made for the accuracy of our AEs, the calculations still clearly overestimate the respective thermochemical threshold values. This is apparent in Figure 1, where the CCSD(T) thresholds are indicated by arrows with dashed lines. In all three cases, the CCSD(T) thresholds occur in the rising edge of the respective peaks and are already about 0.4 - 0.6 eV above the onset. This overestimate is less at the B2PLYP DFT level of theory, which one would *a priori* expect to be the less accurate approach. We note, however, that the values reported here are the reaction enthalpies and as the entropy term is positive in these dissociation reactions, the $-T\Delta S$ contribution to the free energy values, ΔG, shifts these to lower energies as compared to the ΔH values reported here. Nonetheless, the threshold energies calculated here can provide a reliable basis for the interpretation of the low energy contributions. In this context, the low intensity CCl_2^- contribution, peaking at about 1.8 eV, must be attributed to dissociation to CCl_2^- and Cl_2. The higher energy peak at about 6.1 eV, on the other hand, is well above the threshold for dissociation to CCl_2^- and two chlorine atoms, which we consider to be the more likely process at these energies. Likewise the formation of Cl_2^-, peaking at around 1.3 eV, is below the threshold for any further dissociation of the neutral CCl_2 counterpart, although further dissociation through the higher energy contribution peaking at about 6.1 eV cannot be excluded. The same applies for Cl^- formation. In this case it is also worth mentioning that in a recent study by Li *et al*. [75], the energy dependence of the formation of the neutral CCl_3 counterpart was studied in the energy range from about 0 to 3.0 eV and was confirmed to reflect the Cl^- formation at these energies. For completeness, Table 2 lists the adiabatic electron affinities of CCl_n (n = 1-4), Cl and Cl_2 as well as the respective BDEs calculated by us at the B2PLYP and CCSD(T) level of theory. Where available, these results are compared to selected experimentally determined values from the literature.

For the electron affinity of CCl_3 and CCl_2, B2PLYP delivers lower values than the CCSD(T) approach. On the other hand for the respective BDEs; CCl_3–Cl and CCl_2–Cl, B2PLYP is higher

in value in both cases. As the calculated threshold energy values are the difference between these values, they are accordingly lower at the B2PLYP level of theory for both CCl_3^- and CCl_2^-. Comparison with the experimentally determined electron affinity of Cl (see Table 2), which should be a reliable reference, shows that while both approaches overestimate this value, the CCSD(T) result is a little closer in value to the experimental EA. The Cl–Cl BDE, on the other hand, is overestimated by about 0.1 eV at the CCSD(T) level of theory, while the B2PLYP value is about 30 meV below the well-established literature value. Nonetheless, the results embodied within Table 2 do suggest that both present calculations typically do a good job in reproducing the available experimental results. In this context, it is also worth mentioning that recent calculations by Grein [109], at the MP2/6-311 + G(3df) level derive a value of 0.82 eV for the electron affinity of CCl_4. This is 0.08 eV above our CCSD(T) value and 0.05 eV below our B2PLYP value, and therefore in fair agreement with our results.

In summary, Cl^- formation from CCl_4 through DEA in the low energy range (less than about 2 eV) is a well-studied process [48-50, 62, 65], as is discussed in the introduction and here above. Dissociative electron attachment to CCl_4 at higher energies is less studied and the only other energy-calibrated studies reported, with an energy resolution comparable to the current, were conducted by Illenberger's group in the 90's [77-79]. The current observations are in good agreement with results from previous studies, with the exception that neither the dipolar dissociation observed here in the Cl^- ion yield, nor the CCl_3^- contribution at around 6 eV, is reported in those studies by the Illenberger group. Special attention was thus given to these channels and we find that the CCl_3^- contribution at about 6 eV from CCl_4 is very week and depends strongly on the potentials of the ion extraction optics of our setup. We attribute this to the fact that the ions are focused in to the quadrupole mass spectrometer (QMS) through a finite aperture and at low extraction voltages. This causes certain discrimination of fragment ions with high kinetic energy component perpendicular to the extraction axis. This is general for crossed beam setups using a TEM in combination with a QMS and may explain the different observations in the current study as compared to that of the Illenberger's group (for this discrimination effect see e.g. ref. [121]). Similarly, dipolar dissociation (DD) leading to Cl^- was not observed in the previous gas phase study by the Illenberger's group covering the relevant energy range. However, Reese *et al.* [46] report a contribution to the Cl^- yield at around 13 eV in an early study and attributed this contribution to DD. Similarly Craggs and McDowell [122]

report Cl^- formation from CCl_4 with an AE of 12.2 eV and a minimum kinetic energy of 0.5 eV for Cl^- in the process. Furthermore, in electron stimulated desorption (ESD) from CCl_4 condensed on gold surface, a clear, rising Cl^- contribution is observed above about 10 eV, apparently through DD [123]. We note that in the ESD study additional structures are also observed above 6 eV that may additionally contribute to the Cl ion yield in the current study. Most likely this apparent disagreement with the previous study by the Illenberger's group is also due to high kinetic energy release (perpendicular to the extraction axis) in the DD channel. In the current experimental setup, we do not have the means to study the kinetic energy release or the angular dependence in these processes and the setup does not allow for total ion collection. However, the currently available velocity slice imaging or momentum imaging instruments (see e.g. ref. [124] and refs. therein) would be well suited to remove all ambiguity with regards to these ion yields. Finally, we note that the CCl_3^- and Cl^- ion yields shown in Figure 1 are spectra where the best balance between the resolution and ion yield over the full energy range have been achieved.

Overall, we would characterize DEA to CCl_4 as being a well-studied process, offering a fairly complete and consistent picture of low energy electron attachment to CCl_4 in the energy range from about 0 - 10 eV.

3.2 Silicon tetrachloride

Figure 2 shows the energy dependence of the ion yield for all the negative ions we observed upon electron attachment to $SiCl_4$, in the energy range from about 0 to 10 eV. The vertical arrows again denote the appearance energy, as determined by a Wannier fit to the onset region and as outlined in section 2.2

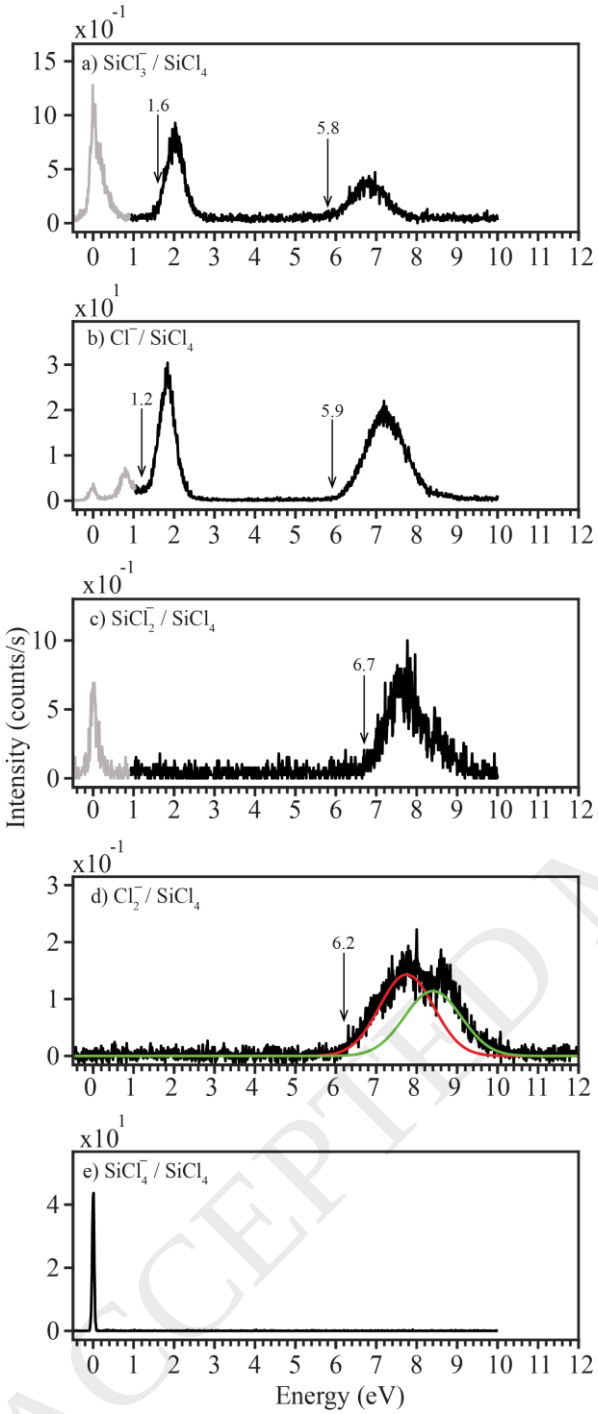

Figure 2. Negative ion yield curves for electron attachment to $SiCl_4$ in the energy range from ~0 to 12 eV. The arrows indicate the appearance energy (eV) determined from the fitting to the rising part of ion yield curves using a Wannier type functional except for Cl^- low energy negative ion yield curve where the appearance energy is determined from the linear fits (see Section 2.2). Intensity on the y axis is normalized to the pressure during the respective measurements. The regions highlighted in grey arise from impurities. See the text for further details.

In Table 3 the appearance energies and the energies of the intensity peak maxima for individual negative ion contributions are listed along with results from the current CCSD(T) and B2PLYP calculations of the thermochemical thresholds; E_{th}, for the formation of the respective ions. In addition to the AE values from the Wannier type fits, those derived by linear fits, as also described in section 2.2 are shown in parenthesis in the Table. For comparison, AEs and peak values reported in earlier energy calibrated studies are also listed in Table 3.

Similar to CCl_4, dissociative electron attachment of $SiCl_4$ leads to the fragments Cl^-, Cl_2^- $SiCl_2^-$ and $SiCl_3^-$. Additionally, the molecular anion $SiCl_4^-$ is observed with an appreciable intensity through a narrow contribution at threshold 0 eV. Note that in Figure 2 the contributions below about 1 eV, in the ion yields for Cl^-, $SiCl_2^-$ and $SiCl_3^-$, are plotted in grey; signifying that we attribute these to impurities formed in the $SiCl_4$ sample during measurements. This latter point is substantiated in more detail below.

From electron attachment to $SiCl_4$, Cl^- and the complementary ion $SiCl_3^-$ are formed through a low energy resonance resulting in distinct maxima in their ion yield curves at 1.8 and 2.1 eV, respectively. At the CCSD(T) level of theory, the thermochemical thresholds for these processes are found to be 1.13 and 1.74 eV, respectively. For Cl^- the CCSD(T) value is lower but in good agreement with the experimentally determined AE. The threshold from the B2PLYP calculation is even lower still (0.77 eV). For the $SiCl_3^-$ formation the calculated thresholds are about 0.1 eV higher than the AE determined with the Wannier fit, which is nonetheless well within the error margins for the respective AEs. In addition to the low energy Cl^- and $SiCl_3^-$ contributions, these ions are also formed from $SiCl_4$ through a broad high-energy contribution peaking at 7.1 eV in the Cl^- yield and at 6.9 eV in the $SiCl_3^-$ yield. The fragments Cl_2^- and $SiCl_2^-$, on the other hand, are only observed through the higher-energy features whereby both fragments exhibit a maximum at around 7.7 eV. The AEs for these contributions, and the low energy features discussed above, agree well with those reported by Jäger *et al*. [90], except for the fact that Jäger *et al*. observe additional contributions in all their ion yields at 0 eV. We attribute these additional signals to impurities formed through hydrolysis of $SiCl_4$, as we discuss later in section 3.2.1, and we do thus not include them in Table 3. The agreement with the AE reported by Wang *et al.* [87] for the Cl^- formation is good for the low energy contribution, but the AE for the high-energy contribution reported by Wang *et al.* is about 0.8 eV higher than the current value. With respect to the energy position of the peak maxima, however, the agreement is generally marginal (see

Table 3). While there is a fair agreement with most of the values reported by Jäger *et al*. [90], all of Jäger *et al*. [90], Wang *et al* [87] and Moylan *et al*. [89] show the $SiCl_4^-$ formation to peak significantly above threshold, i.e., at 0.5, 0.3 eV and 2 eV respectively, whereas we find it to be at 0 eV. The peaks of the higher energy contributions determined in these earlier studies are also generally somewhat higher in energy than those reported here, though the present peak maximum for the low energy Cl^- formation at about 1.8 eV agrees well with all those studies as well as with that of Pabst *et al*. [88].

Wan *et al*. [80] reported ETS, and TCS data, for all of the chloro- and teterahalo-silanes in 1989. For $SiCl_4$ their ETS shows a weak but distinct resonance close to 1.3 eV, two prominent resonances at 2.2 eV and at about 5.5 eV, respectively, and a broad less distinct resonance close to 9 eV. Note that in their TCS the 1.3 eV resonance appears as a low-energy shoulder on the prominent 2.2 eV peak. The authors assign the 2.2 eV contribution to the t_2 symmetry LUMO+1, but the 1.3 eV feature and the higher-energy resonances at about 5.5 and 9 eV are left unassigned. In conjunction with the 1.3 eV contribution, the authors [80] point out that the total symmetric a_1 orbital does not give rise to a centrifugal barrier and should thus not appear in ETS above threshold. Further, they conjectured that splitting of the triply degenerate t_2 orbital might be a possible source of the low energy contribution in the ETS. However, based on quantum chemical calculations, they conclude that this splitting would be insufficient to support that interpretation. In a later publication by the same group [125] this assignment is revisited in conjunction with electron impact inner shell excitation of the chlorosilanes, including $SiCl_4$. Based on their inner shell excitations (and in light of previous observations of ETS features associated with the a_1 orbitals in halogenated compounds) the authors reassigned the 1.3 eV resonance to the a_1 LUMO of $SiCl_4$. In a later study, Modelli et al. [74] reported ETS and ion yield curves for $SiCl_4$ along with results from MS-Xα calculations. In good agreement with the previous ETS, they observe resonant contributions at 1.15, 2.07 and at 5.4 eV and assign the former two contributions to single electron occupation of the a_1 LUMO and t_2 LUMO+1, respectively. These assignments are supported by their MS-Xα calculations, which place these resonances at 0.9 and 2.3 eV respectively. Further, in their ion yield they observe a dominant formation of $SiCl_4^-$ at threshold (0 eV incident electron energy), which they also associate with a single electron occupation of the a_1 LUMO mediated by the rapid increase of the capture cross section near 0 eV. In a more recent study, Bettega et al. [83] report SMC results on the elastic

integral, differential and momentum transfer cross sections for low-energy electron collisions with $SiCl_4$ using the static-exchange and static-exchange (SE) plus polarization (SEP) approximations. In the SE approach resonant enhancements belonging to the A_1, T_2, and E symmetries are computed at 3, 4, and 8 eV, but in the SEP approach the A_1 contribution becomes a bound state and the T_2 and E contributions are shifted to about 2 and 6 eV, respectively. This is in good agreement with the location of these resonances in the ETS spectra, assuming that the 5.4 eV ETS contribution corresponds to the E symmetry component in the SEP calculations. With respect to the resonance positions, their agreement [83] with the experimental TCS of Wan *et al.* [80] and Mozejko *et al.* [81] is also good. Furthermore, in conjunction with the sharp rise in the s-wave cross section observed in their calculations at low energies and the dominant $SiCl_4^-$ threshold contribution observed by Moelly et al. [74], Bettega et al. [83] have explored the potential presence of a virtual state enabling s-wave attachment at threshold. In fact, from their calculations of the s-wave eigenphase at very low energies, they derive large negative numbers for the scattering length, i.e., values that support the presence of a virtual state at threshold.

According to these studies we can safely assign the 1.8 and 2.1 eV features in the ion yields of Cl^- and $SiCl_3^-$, respectively, to a single electron shape resonance associated with the σ*(Si-Cl), t_2 LUMO+1. Correspondingly, the $SiCl_4^-$ threshold contribution must be ascribed to s-wave attachment associated with the a_1 LUMO. In the current DEA spectra the Cl^- ion yield is shifted to lower energies compared to the location of the T_2 resonance in the ETS, while the maximum in the $SiCl_3^-$ ion yield is at a comparable energy to that of the T_2 resonance. This is likely to result from the energy dependence of the branching ratio of the respective resonance with respect to dissociation paths and survival probability [97]. In that respect, we note that the thermochemical threshold for Cl^- formation is at 1.15 eV while that for $SiCl_3^-$ formation is 1.67 eV. The assignment of the high-energy contributions that exhibit peaks in the energy range from 6.9 to 7.7 eV, in the Cl^-, $SiCl_3^-$, $SiCl_2^-$ and Cl_2^- ion yields from $SiCl_4$, is not as straight forward. These contributions appear well above the energy of the E symmetry shape resonance observed at about 6 eV in the SMC-SEP calculations, and well above the resonant structures observed in the ETS and the experimental TCS, which appear at 5.4 eV and about 5.5 eV, respectively [74, 81]. The DEA features in the range from 6.9 to 7.7 eV are thus more likely to arise from core excited resonances associated with electronic excitations from higher lying valence orbitals, such as the bonding t_1 and t_2 HOMOs to either the a_1 or t_2 LUMOs. From photoabsorption [126] and

X-ray inner electron spectra of $SiCl_4$ [127], the energy difference between the HOMO and LUMO is found to be around 6.2 eV.

In, Table 4 we show the electron affinities of $SiCl_n$ (n = 1-4) and the BDEs for $SiCl_n$−Cl (n = 0 - 3), calculated again at the CCSD(T) and B2PLYP level of theory. Our calculated BDE values agree well with the experimental values reported in the literature, except for Si−Cl where our results are more than 1 eV higher. Experimentally determined EA values for $SiCl_4$ and its fragments, on the other hand, are very limited in numbers, and we are only aware of estimates from Pabst *et al*. [88], for $SiCl_2$ and $SiCl_3$, and a lower limit for $SiCl_2$ from a very early study by Vought *et al*. [85]. All those values are in poor agreement with the calculated results reported here. In addition to these, a vertical electron affinity has been determined for $SiCl_4$ by Hatano and Ito [128] and it is also presented in Table 4. Finally, we note that Grein *et al.* [109] have calculated the adiabatic EA of $SiCl_4$ at the MP2/6-311 + G(3df) level of theory and find it to be 0.47 eV. This value agrees fairly well with our B2PLYP calculations (0.40 eV) but is more than 0.3 eV higher than the value we obtain at the CCSD(T) level.

3.2.1 Impurities formed during the measurements, inconsistency of the previous measurements.

In addition to the contributions discussed above, we also observe significant 0 eV features in the yields of $SiCl_2^-$ and $SiCl_3^-$ as well as contributions at about 0 and 0.8 eV in the Cl^- ion yield. These contributions are all well below the thermochemical thresholds we calculated for these fragments, when formed from $SiCl_4$. Furthermore, for $SiCl_2^-$and $SiCl_3^-$ their intensity was found to increase with increasing measurement time. This indicates that these features originate from degradation products formed from $SiCl_4$ during the measurements. This is clearly documented in Figures 3, 4 and 5 which show the ion yield curves for $SiCl_2^-$, $SiCl_3^-$ and Cl^-, respectively, for repeated scans over a time period of 1 hour, 3 hours and 3.5 hours, respectively. For $SiCl_2^-$ and $SiCl_3^-$ the 0 eV contribution is marginal in the first scan, but it is absolutely dominant for $SiCl_2^-$ and very significant for $SiCl_3^-$ by the time the last scan is recorded.

As discussed in the introduction, previous measurements on DEA to $SiCl_4$ give results that are sometimes quite contradictory. We believe that the dramatically different product distributions observed originates through the decomposition of $SiCl_4$. To examine this idea, we performed a negative ion mass scan for the higher masses, with 0 eV electron incident energy (not shown here). We observed the formation of higher masses like Si_2Cl_6, Si_2Cl_5, Si_2Cl_4, $SiCl_3O$, Si_2Cl_6O

and Si_2Cl_5O. The thresholds for the formation of $SiCl_3^-$ from Si_2Cl_6, Si_2Cl_5 and Si_2Cl_5OH are 0.33, -1.34 and -2.17 eV respectively. Similarly, the thresholds for the formation of $SiCl_2^-$ from Si_2Cl_6, Si_2Cl_4 and Si_2Cl_5OH are respectively 0.24, -0.592 and -2.38 eV (calculated at the B2PLYP level of theory). Hydrolysis of chlorosilanes is a very efficient process that may lead to dimerization/oligomerization of the intermediates. As a consequence, the low energy contributions in the $SiCl_3^-$ and $SiCl_2^-$ ion yields are attributed to DEA reactions of hydrolysis products formed through reactions of $SiCl_4$ with residual water in the inlet system.

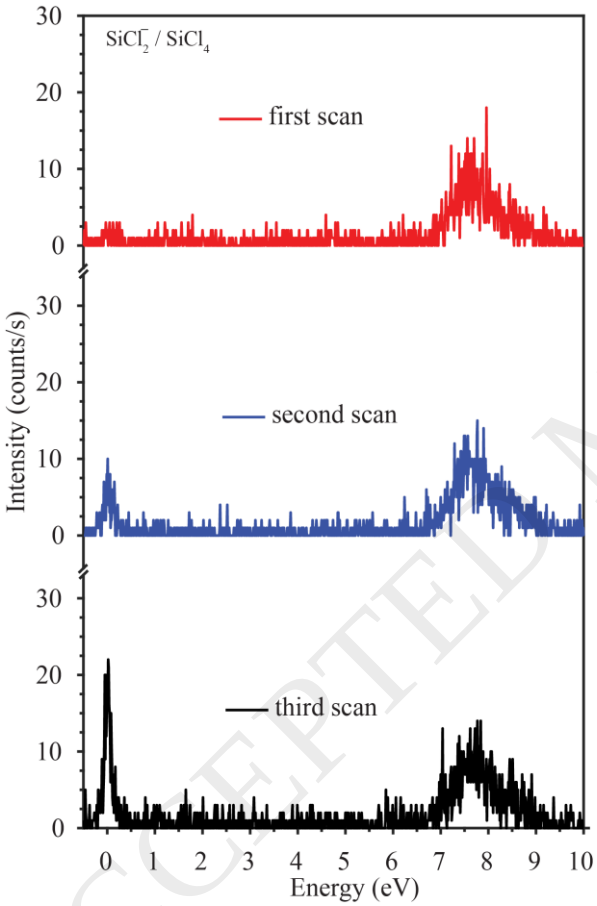

Figure 3. Progressive negative ion yield curves showing the formation of $SiCl_2^-$ recorded over a total time of 1 hour. The 0 eV contribution is absent in the first scan, but is the most significant in the last scan, while the high-energy contribution at about 7.5 eV stays constant over this time period.

Similarly the low energy contribution at about 0.8 eV in the Cl^- ion yield is attributed to DEA of HCl [59], also formed through hydrolysis of $SiCl_4$. This process, however, displays no obvious time dependence (see Figure 5). We attribute this later observation to the relatively high vapour pressure of HCl and the comparatively low cross section for Cl^- formation from HCl at 0.8 eV

[59].

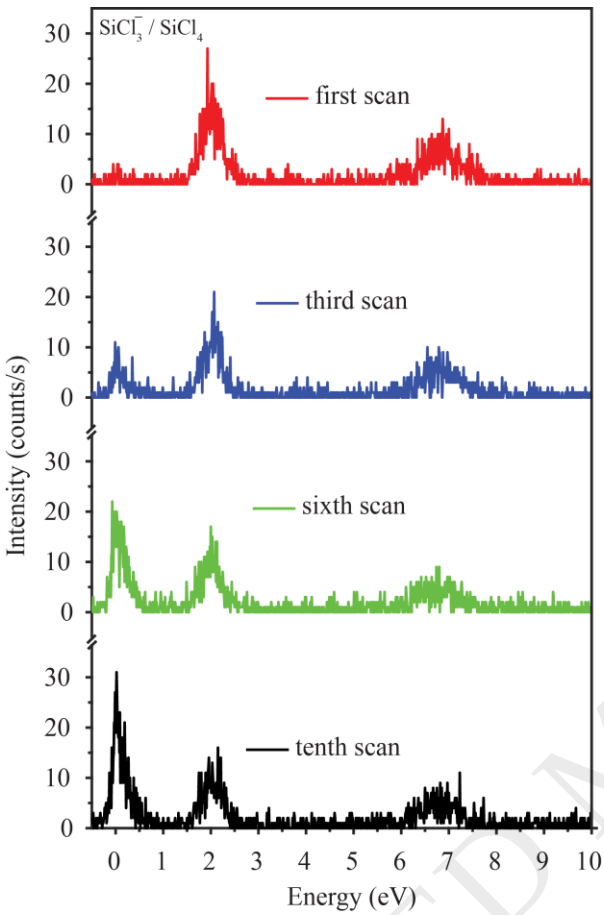

Figure 4. Progressive negative ion yield curves showing the formation of $SiCl_3^-$ recorded over a total time of 3.0 hours. The 0 eV contribution is absent in the first scan, but is the most significant in the last scan. On the other hand the high energy contributions at about 2 and 7.5 eV stay relatively constant.

This follows as the former provides a relatively stable partial pressure, while the latter hampers observation of the effect of any small partial pressure changes on the ion yield. Finally the low intensity 0 eV contribution in the Cl^- ion yield also does not show the same time dependency as was observed for $SiCl_3^-$ and $SiCl_2^-$, and the thresholds for the formation of Cl^- from the high mass hydrolysis products are in all cases well above 0 eV. Considering the exceptionally high cross section for Cl^- formation from CCl_4 at 0 eV incident electron energies, we consider it most likely that this signal results from trace amounts of CCl_4 contributing to the $SiCl_4$ measurement, through either the sample or inlet system. For the current signal intensity observed, these impurities do not have to exceed 0.0005 % to explain the 0 eV contribution in Figure 5.

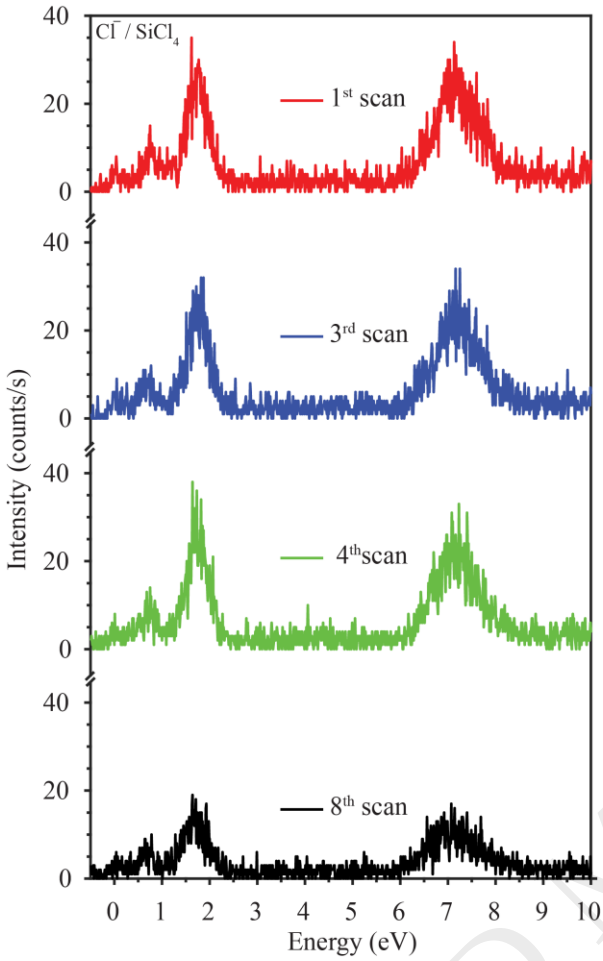

Figure 5. Progressive negative ion yield curves showing the formation of Cl^- recorded over a total time of 3.5 hours. The 0.8 eV contribution is attributed to HCl formed through hydrolysis of $SiCl_4$, while the 0 eV contribution is attributed to traces of CCl_4.

In summary, several DEA studies on $SiCl_4$ have been previously conducted and indeed they date back to 1947. These studies, however, are all incomplete in one-way or another, and their results do not generally agree. In the current study, the experiments were conducted under well-defined single collision conditions and the relevant energy range from 0-12 eV was covered with an energy resolution of about 120 meV and high sensitivity. We can thus offer the first complete and consistent picture of the DEA processes induced in $SiCl_4$, in the relevant energy range, and we can correlate our results to resonance structures observed in previous scattering studies and predicted by theory. Furthermore, through comparison with calculated thermochemical thresholds and the examination of high mass fragments, we can offer a plausible explanation for some of the inconsistencies found between the earlier experiments.

3.3. Germanium tetrachloride

Figure 6 shows the energy dependence of the ion yield for all negative ions observed upon electron attachment to $GeCl_4$, in the energy range from about 0 to 10 eV. As was the case previously, the vertical arrows show the appearance energy, determined by fitting a Wannier type function to the onset of the ion yields, as outlined in section 2.2. In Table 5 the appearance energies and the energies of the peak maxima for the individual negative ion contributions are listed, along with the current CCSD(T) and B2PLYP DFT calculation results of the thermochemical thresholds; E_{th}, for the formation of the respective ions. The respective AEs derived from a linear fit (also see section 2.2) are shown in parenthesis. For comparison, appearance energies and energy peak values available from earlier energy calibrated studies are also listed in the table.

Similar to CCl_4 and $SiCl_4$, dissociative electron attachment to $GeCl_4$ leads to formation of the fragments Cl^-, Cl_2^-, $GeCl_2^-$ and $GeCl_3^-$. Here, we find that the most significant contribution is through $GeCl_3^-$ formation at about 0 eV (see Figure 6). Further contributions to the $GeCl_3^-$ ion yield are observed at about 1.4 eV and at about 5.0 eV. Both of these contributions are fairly narrow, the former with a FWHM of about 0.5 eV, the latter with a FWHM of about 1.4 eV. Significant intensity is also observed in the Cl^- channel from $GeCl_4$, but only through the broad higher lying resonance. This contribution peaks at about 5.5 eV, and noticeably the intensity of this peak is about a third of that of the 0 eV contribution in the $GeCl_3^-$ ion yield. This is unusual as the attachment cross section for a given anion is normally significantly higher close to 0 eV, where the energy dependency of the attachment cross section is proportional to $E^{-1/2}$ [97]. Further, low intensity contributions are visible in the Cl^- ion yield at about 0 eV and about 0.8 eV (shown in grey in the top panel of Figure 6). We, however, attribute the former of these features to residual CCl_4 in the inlet system, and the latter to electron attachment to HCl [59] formed through hydrolysis of $GeCl_4$. The origin of these impurities, and their significance, was discussed for $SiCl_4$ above and the same rationale applies here for $GeCl_4$. The fragments Cl_2^- and $GeCl_2^-$ are also formed through the high-energy resonance, but with an intensity more than 2 orders of magnitude lower than that for the Cl^- yield through the same resonance. For Cl_2^- the maximum intensity is at about 6 eV, while the maximum intensity for $GeCl_2^-$ production is at about 5.7 eV.

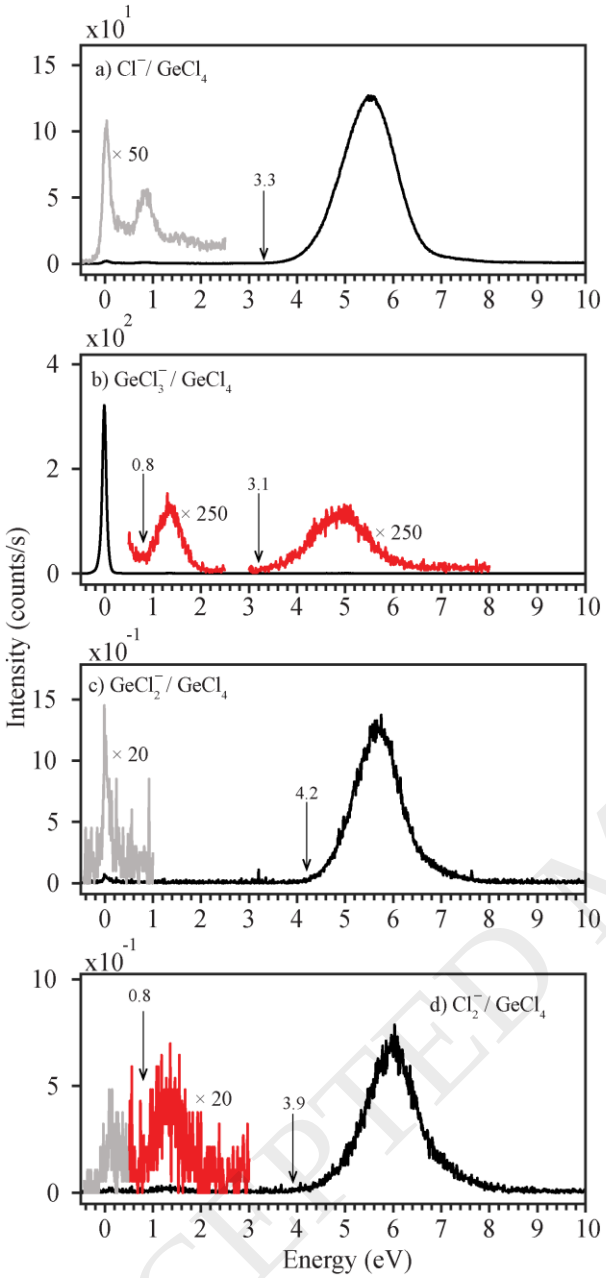

Figure 6. Negative ion yield curves for electron attachment to $GeCl_4$ in the energy range from ~0 to 10 eV. The arrows indicate the appearance energy (eV) determined from fitting the rising part of ion yield curves using a Wannier type fitting function except for the $GeCl_3^-$ and Cl_2^- low energy ion yield curve where the appearance energy is determined from the linear fits (see Section 2.2). The intensity is normalized with regards to the pressure during the measurements.

Finally, $GeCl_2^-$ is also produced, though with very low intensity, through a contribution with a maximum at about 1.3 eV. Marginal 0 eV contributions are also observed in the ion yields for $GeCl_2^-$ and Cl_2^-. In the former case we attribute this contribution to residues of the SF_6 calibration gas leading to SF_6^- formation, which has the *m/z* ratio of 146. The origin of the 0 eV

contribution in the Cl_2^- ion yield is not clear, but for these very small intensities we consider electron attachment to decomposition products formed at the hot cathode to be the most likely explanation.

According to our CCSD(T) calculations, the formation of $GeCl_3^-$ is endothermic by about 0.3 eV while at the B2PLYP level of theory it is endothermic by about 0.1 eV (see Table 5). From the ion yield curves, on the other hand, it is clear that this process is exothermic and that the calculated thresholds are an overestimate, particularly at the CCSD(T) level of theory. The AE for the low energy contribution in the Cl_2^- yield is also below the CCSD(T) threshold value. The intensity of this contribution is, however, very low and thus not allowing the exclusion of a proportionally significant contribution through the high energy tail of the Maxwell Boltzmann distribution of internal energies, i.e., hot band transitions. The AEs of all the other fragments observed in DEA to $GeCl_4$ are well above their threshold, restricting our ability to further compare the AEs between experiment and theory. Table 5 also compares the current AEs, with those reported by Guillot *et al*. [92], and the energies of peak intensity maxima values estimated from Pabst *et al*. [88], Guillot *et al.* [92] and Modelli *et al.* [74].

In the early study by Pabst *et al*. [88], the formation of Cl^-, Cl_2^- $GeCl_2^-$ and $GeCl_3^-$, through a broad contribution appearing with a maximum in the ion yield curves in the range from about 5.5-6.5 eV, is reported. With the exception of the $GeCl_3^-$ ion yield, the energy range above 1 eV is only considered in their study. In the $GeCl_3^-$ ion yield, Pabst *et al*. [88] also observe a contribution at around 2 eV, which most likely corresponds to the 1.3 eV contribution observed in the current study. The significant 0 eV $GeCl_3^-$ contribution observed here is not reported by Pabst *et al*. [88], and neither is the low intensity Cl_2^- contribution at about 1.3 eV. The differences between the current observations and those by Pabst *et al*. [88] are most significant in the low energy range, and most likely are rooted in the poorly defined electron energy in their study and limitations of their instrumentation in respect to the formation and detection of negative ions at very low energies, i.e., in the range around 0 eV.

In a later ETS and DEA study, Guillot *et al.* [92] report the observation of two resonances in their ETS spectra, the former at 1.72 eV and the latter at about 5.6 eV. In DEA they observe the formation of $GeCl_3^-$ through a narrow contribution at 0 eV, and the formation of Cl^- and $GeCl_2^-$ with peak maxima at 5.5 eV and 5.7 eV respectively. While both $GeCl_3^-$ and Cl^- are produced with appreciable intensity, the $GeCl_2^-$ contribution is only minor and no contributions are

observed through the resonance located at 1.72 eV in their ETS. In a later publication by Modelli *et al*. [74] these findings are confirmed, and the reported relative scale DEA intensities of the fragments observed in the previous study are corrected and reported to be in the ratio 100:94:10 for $GeCl_3^-$, Cl^- and $GeCl_2^-$. This is qualitatively in fair agreement with the corresponding 100:45:1 ratios observed here. In the studies by Modelli *et al* [74] and Guillot *et. al* [92] the authors assign the ETS 1.72 eV resonance to a single electron occupation of the triply degenerated, t_2-symmetry LUMO+1, which is in good agreement with their MS-Xα calculations that placed this resonance at 1.7 eV. The 0 eV contribution is attributed to single electron occupation of the a_1 LUMO, which their MS-Xα calculations predict to be 0.6 eV below the ground state neutral species. We, however, note that Guillot *et. al* [92] also offer an alternative explanation for the 0 eV $GeCl_3^-$ contribution. That explanation stems from the low energy tail of the T_2 resonance associated with the triply degenerate LUMO+1. The resonance they observed at 5.6 eV in the ETS, and is exhibited in their Cl^- and $GeCl_2^-$ ion yields at 5.5 and 5.7 eV respectively, is discussed in relation to its FWHM, which is reported to be about 1.1 eV. This is quite narrow considering the relatively high energy of this resonance, which indicates a fairly long lived, possibly a closed-channel core excited, resonance. However, these authors [92] point out that this feature may also be associated with a high barrier single particle shape resonance with predominant Ge *d*-orbital character, i.e., l = 2. They further note that this interpretation would be in agreement with single electron occupation of an e-symmetry (6e), predominantly Ge-*d* character orbital, as identified in their X-ray spectra.

Finally, Table 6 shows the electron affinities of $GeCl_n$ (n = 1-4) and the BDEs for $GeCl_n$−Cl (n = 0 -3) calculated at the CCSD(T) and B2PLYP level of theory. Similar to $SiCl_4$, experimentally determined EA values for $GeCl_4$ and its fragments, are very limited. We are only aware of the estimates from Pabst *et al*. [88] for $GeCl_2$ and $GeCl_3$, and a lower limit for $GeCl_2$ reported from a very early study by Vought *et al*. [85]. As is the case for $SiCl_4$, all these earlier values are in poor agreement with the calculated values reported here for $GeCl_4$. In addition, the vertical EA of $GeCl_4$ reported by Hatano and Ito [128] is also shown in Table 6. Finally, in their calculations at the MP2/6-311 + G(3df) level of theory, Grein [109] finds the adiabatic EA of $GeCl_4$ to be 1.43 eV, which is about 0.4 eV lower than our B2PLYP value (1.80 eV) and about 0.1 eV lower than our CCSD(T) value.

4. Conclusions

As a part of our effort to characterise the electron attachment reactions of the group IV tetrahalides, the present work has reported electron attachment to the group IV tetrachlorides: XCl_4 (X = C, Si and Ge) in the energy range from about 0 - 10 eV. We have further determined the AEs of individual fragments and we compare these to the respective threshold energies calculated at the B2PLYP and the CCSD(T) level of theory. We have also provided an extensive literature review on the presently available electron attachment investigations, experimental and theoretical electron scattering studies and on electron transmission studies of these molecules. The electron attachment reactions observed were discussed in relation to these previous studies in an attempt to give a complete and consistent picture of the reactions of these molecules upon electron attachment.

The current work on CCl_4 is consistent with results from previous studies, already offering a fairly complete picture of the observed electron attachment and dissociation processes. Electron attachment to CCl_4 in the energy range from about 0-10 eV is characterized by the formation of Cl^-, Cl_2^-, CCl_2^- and CCl_3^-. These are formed through three resonances appearing in the ion yields through maxima at 0 eV, 0.8-1.8 eV and around 6 eV. The 0 eV contribution is only apparent in the Cl^- ion yield and is attributed to a single particle resonance associated with the a_1-symmetry LUMO. The contributions peaking between 0.8 and 1.8 eV, are apparent in the ion yields of all fragments and are assigned to a single particle shape resonance associated with occupation of the t_2-symmetry LUMO+1. Finally, the contribution at around 6 eV, also apparent in the ion yield of all fragments, is associated with a single particle resonance of e-symmetry. These assignments are derived with support from previous scattering and ETS studies and calculations. The absence of CCl_3^- contribution at about 6 eV and Cl^- formation through DD in most of the previous studies we attribute to the discrimination of fragments with high kinetic energy component perpendicular to the extraction axis and high kinetic energy release in the process. We propose studies with velocity slice imaging or momentum imaging instruments to remove these ambiguities with regards to CCl_3^- and Cl^- ion yields.

For $SiCl_4$ the earlier electron attachment studies have been incomplete and contradictory. Here we have presented a complete and consistent picture of electron attachment to this molecule and we have offered an explanation for the inconsistency between the previous studies. Similar to CCl_4, electron attachment to $SiCl_4$ leads to the formation of the fragment anions Cl^-, Cl_2^-, $SiCl_2^-$

and $SiCl_3^-$. Additionally, the molecular anion $SiCl_4^-$, is observed with appreciable intensity at 0 eV. No fragmentation is observed at such low energies. Based on ETS and Xα calculations [74], we attribute the formation of the molecular anion to a single particle resonance associated with the a_1 LUMO of this molecule. According to the ETS, this state lies 1.15 eV above threshold and the formation of the molecular ion at 0 eV is anticipated to be through a virtual state at threshold. This assertion is substantiated through converged coupled-channel calculations by Bettega *et al*. [83]. All fragments formed upon DEA to $SiCl_4$ are observed through features peaking in the energy range from 6.9-7.7 eV and Cl^- and $SiCl_3^-$ are also observed through appreciable contributions peaking close to 2 eV. We assign the contributions at around 2 eV to a single particle shape resonance associated with the t_2 LUMO+1, observed in the ETS at 2.07 eV. The high energy contributions peaking in the energy range from 6.9-7.7 eV are however well above the e-symmetry resonance observed in the ETS and TCS. As a consequence they are tentatively assigned to core excited resonances associated with HOMO-LUMO transitions.

With regard to the inconsistencies in the results from previous studies, we have shown that even if utmost care is taken, $SiCl_4$ is subject to hydrolysis in our inlet system, leading to dimerization and silicon ether formation (presumably also oligomerization). The formation of $SiCl_2^-$ and $SiCl_3^-$ from these compounds through DEA is exothermic, leading to their observation at threshold, in the current and in previous studies, with the significance of these contributions depending strongly on the experimental conditions.

For $GeCl_4$ the picture is again similar, with electron attachment leading to the formation of Cl^-, Cl_2^-, $GeCl_2^-$ and $GeCl_3^-$. From these, $GeCl_3^-$ is formed through a significant contribution at 0 eV and through a feature peaking at about 1.3 eV. The fragment Cl_2^- also shows a low intensity contribution peaking at ≈1.4 eV, and all these fragments are additionally formed through higher energy contributions peaking in the energy range from about 5 to 6 eV. Leaning on the results from Xα calculations and ETS, we assign the first contribution to a single particle resonance associated with the a_1 LUMO and the second to the t_2 LUMO+1. The assignment of the high-energy contributions is not as straight forward, but these are in good agreement with the 5.6 eV feature observed in the ETS study where it was assigned as an e-symmetry shape resonance with significant Ge-*d* character [92]. The strong atomic *d*-character, and thus the comparably long life time, of this resonance is apparently reflected in its width in the ETS, and is in agreement with the significant contribution we observe in the Cl^- ion yield at around 5.5 eV. However, we note

that at this time we can by no means exclude contributions from core-excited resonances associated with HOMO-LUMO transitions.

Though the current picture of electron attachment and negative ion formation from these compounds is consistent and must be considered fairly complete, there are still ambiguities with regards to the assignment of individual contributions to the respective resonances. These ambiguities may be clarified through techniques such as velocity slice imaging and momentum imaging of the angular dependency of the DEA process, see for example refs. [22, 132] and references therein.

Finally, we found that our calculations at the B2PLYP and CCSD(T) level of theory generally overestimated the thresholds for the respective DEA processes. This is more significant at the CCSD(T) level of theory and most apparent for DEA channels observed for CCl_4. Nonetheless, these discrepancies are generally not very significant and judging from the experimental values for CCl_4 they are mainly rooted in an underestimate of the EAs of the fragments. However, in some cases they also arise from overestimates of the BDEs. Nevertheless we consider our calculated EAs and BDEs to be generally accurate to within 0.2 to 0.3 eV, and in many cases to be better than these estimations. For most of the channels reported here these values are thus the most accurate available in the literature today.

Acknowledgements

This work was conducted under the support of the Icelandic Center of Research (RANNIS; Grants No. 13049305 and 141218051), the University of Iceland Research Fund, the Australian Research Council through the grant DP160102787 and the Japanese Ministry of Education, Sport, Culture and Technology. OI acknowledges financial support from the ARC Centre of Excellence for Antimatter-Matter Studies, for his visit to Flinders University in 2012, and the College of Science and Engineering at Flinders for his 2017 Visiting Research Fellowship. RKTP thanks the University of Iceland Research Fund for the award doctoral grant. PL-V acknowledges the Portuguese National Funding Agency FCT-MCTES research grant PEst-OE/FIS/UI0068/2013 and his Visiting Professor position at Sophia University, Tokyo, Japan

References.

[1] E. H. Bjarnason, F. H. Ómarsson, M. Hoshino, H. Tanaka, M. J. Brunger, P. Limão-Vieira, O. Ingólfsson, Negative ion formation through dissociative electron attachment to the group IV tetrafluorides: Carbon tetrafluoride, silicon tetrafluoride and germanium tetrafluoride, International Journal of Mass Spectrometry, 339 (2013) 45-53.
[2] F. H. Ómarsson, B. Reynisson, M. J. Brunger, M. Hoshino, H. Tanaka, P. Limão-Vieira, O. Ingólfsson, Negative ion formation through dissociative electron attachment to the group IV tetrabromides: Carbon tetrabromide, silicon tetrabromide and germanium tetrabromide, International Journal of Mass Spectrometry, 365 (2014) 275-280.
[3] V. Regnault, Sur les chlorures de carbone CCl et CCl_2, in: Annales de Chimie et de Physique, 1839, pp. 104-107.
[4] E. M. Davidson, Process of extinguishing fires, in, Pyrene Mfg Co, US, 1911.
[5] R. E. Doherty, A history of the production and use of carbon tetrachloride, tetrachloroethylene, trichloroethylene and 1, 1, 1-trichloroethane in the United States: Part 1--historical background; carbon tetrachloride and tetrachloroethylene, Environmental Forensics, 1 (2000) 69-81.
[6] M. A. Lieberman, A. J. Lichtenberg, Principles of plasma discharges and materials processing, John Wiley & Sons, 2005.
[7] The Montreal Protocol on Substances that Deplete the Ozone Layer, 1987, http://ozone.unep.org/en/handbook-montreal-protocol-substances-deplete-ozone-layer/27571
[8] WMO (World Meteorological Organization), *Scientific Assessment of Ozone Depletion: 2010*, Global Ozone Research and Monitoring Project-Report No. 52, 516, Geneva, Switzerland, 2011.
[9] A. Benami, G. Santana, A. Ortiz, A. Ponce, D. Romeu, J. Aguilar-Hernández, G. Contreras-Puente, J. Alonso, Strong white and blue photoluminescence from silicon nanocrystals in SiN_x grown by remote PECVD using $SiCl_4/NH_3$, Nanotechnology, 18 (2007) 155704.
[10] O. Sanchez, J. M. Martinez-Duart, R. J. Gomez-Sanroman, R. Perez-Casero, M. A. Aguilar, C. Falcony, F. Fernandez-Gutierrez, M. Hernández-Vélez, SiO_xN_y Films deposited with $SiCl_4$ by remote plasma enhanced CVD, Journal of Materials Science, 34 (1999) 3007-3012.
[11] P. Woditsch, W. Koch, Solar grade silicon feedstock supply for PV industry, Solar Energy Materials and Solar Cells, 72 (2002) 11-26.
[12] A. F. B. Braga, S. P. Moreira, P. R. Zampieri, J. M. G. Bacchin, P. R. Mei, New processes for the production of solar-grade polycrystalline silicon: A review, Solar Energy Materials and Solar Cells, 92 (2008) 418-424.
[13] W. G. French, J. B. MacChesney, A. D. Pearson, Glass fibers for optical communications, Annual Review of Materials Science, 5 (1975) 373-394.
[14] L. Sun, K. Gong, Silicon-based materials from rice husks and their applications, Industrial & Engineering Chemistry Research, 40 (2001) 5861-5877, and references therein.
[15] J. M. Chen, F. W. Chang, The chlorination kinetics of rice husk, Industrial & Engineering Chemistry Research, 30 (1991) 2241-2247.
[16] D. W. Lyon, C. M. Olson, E. D. Lewis, Preparation of Hyper-Pure Silicon, Journal of The Electrochemical Society, 96 (1949) 359-363.
[17] S. Sakaguchi, S.-I. Todoroki, Optical properties of GeO_2 glass and optical fibers, Applied Optics, 36 (1997) 6809-6814.
[18] C. C. Huang, D. W. Hewak, High-purity germanium-sulphide glass for optoelectronic applications synthesised by chemical vapour deposition, Electronics Letters, 40 (2004) 1.
[19] J. E. Huffman, N. L. Casey, Growth methods for high purity Ge and Ge: Ga homoepitaxy, Journal of Crystal Growth, 129 (1993) 525-531.

[20] S. G. Kukolich, Demonstration of the Ramsauer-Townsend effect in a Xenon thyratron, American Journal of Physics, 36 (1968) 701-703.
[21] H. Hotop, M.-W. Ruf, M. Allan, I. I. Fabrikant, Resonance and threshold phenomena in low-energy electron collisions with molecules and clusters, Advances in Atomic, Molecular, and Optical Physics, 49 (2003) 85-216.
[22] I. I. Fabrikant, S. Eden, N. J. Mason, J. Fedor, Chapter Nine - Recent Progress in Dissociative Electron Attachment: From Diatomics to Biomolecules, in: C.C.L. Ennio Arimondo, F.Y. Susanne (Eds.) Advances In Atomic, Molecular, and Optical Physics, Academic Press, 2017, pp. 545-657.
[23] I. Bald, J. Langer, P. Tegeder, O. Ingólfsson, From isolated molecules through clusters and condensates to the building blocks of life, International Journal of Mass Spectrometry, 277 (2008) 4-25.
[24] O. Ingólfsson, F. Weik, E. Illenberger, The reactivity of slow electrons with molecules at different degrees of aggregation: gas phase, clusters and condensed phase, International Journal of Mass Spectrometry and Ion Processes, 155 (1996) 1-68.
[25] J. H. W. Holst, Kgl. Nor. Vidensk. Selsk, 4 (1931) 89.
[26] C. Szmytkowski, A. M. Krzysztofowicz, P. Janicki, L. Rosenthal, Electron scattering from CF_4 and CCl_4. Total cross section measurements, Chemical Physics Letters, 199 (1992) 191-197.
[27] A. Hamada, O. Sueoka, Total cross-section measurements for positrons and electrons colliding with molecules: CCl_4, Applied Surface Science, 85 (1995) 64-68.
[28] R. K. Jones, Absolute total cross sections for the scattering of low energy electrons by CCl_4, CCl_3F, CCl_2F_2, $CClF_3$, and CF_4, The Journal of Chemical Physics, 84 (1986) 813-819.
[29] H. X. Wan, J. H. Moore, J. A. Tossell, Electron attachment to the chlorosilanes and chloromethanes, The Journal of Chemical Physics, 94 (1991) 1868-1874.
[30] A. Zecca, G. P. Karwasz, R. S. Brusa, Absolute total-cross-section measurements for intermediate-energy electron scattering on CF_4, $CClF_3$, CCl_2F_2, CCl_3F, and CCl_4, Physical Review A, 46 (1992) 3877.
[31] G. P. Karwasz, R. S. Brusa, A. Zecca, 6.1 Total scattering cross sections, in: Interactions of Photons and Electrons with Molecules, Springer, 2003, pp. 6001-6051.
[32] J. Randell, J. Ziesel, S. L. Lunt, G. Mrotzek, D. Field, Low energy electron scattering by CF_3Cl, CF_2Cl_2, $CFCl_3$ and CCl_4, Journal of Physics B: Atomic, Molecular and Optical Physics, 26 (1993) 3423.
[33] A. P. P. Natalense, M. H. F. Bettega, L. G. Ferreira, M. A. P. Lima, Low-energy electron scattering by CF_4, CCl_4, $SiCl_4$, $SiBr_4$, and SiI_4, Physical Review A, 52 (1995) R1.
[34] A. P. P. Natalense, M. T. D. N. Varella, M. H. F. Bettega, L. G. Ferreira, M. A. P. Lima, Applications of the Schwinger multichannel method with pseudopotentials to electron scattering from polyatomic molecules I: elastic cross sections, Brazilian Journal of Physics, 31 (2001) 15-20.
[35] M. T. D. N. Varella, A. P. P. Natalense, M. H. F. Bettega, M. A. P. Lima, Low-energy electron scattering by CF_4, CCl_4, $SiCl_4$, $SiBr_4$, and SiI_4, Physical Review A, 60 (1999) 3684.
[36] D. L. Azevedo, M. H. F. Bettega, L. G. Ferreira, M. A. P. Lima, Scattering of low-energy electrons by $TiCl_4$, $GeCl_4$, $SiCl_4$ and CCl_4: a comparison of elastic cross sections, Journal of Physics B: Atomic, Molecular and Optical Physics, 33 (2000) 5467.
[37] G. M. Moreira, A. S. Barbosa, D. F. Pastega, M. H. F. Bettega, Low-energy electron scattering by carbon tetrachloride, Journal of Physics B: Atomic, Molecular and Optical Physics, 49 (2016) 035202.
[38] M. Heng, S. De-Heng, S. Jin-Feng, L. Yu-Fang, Z. Zun-Lue, A Modified Potential Method for Electrons Scattering Total Cross Section Calculations on Several Molecules at 30~ 5000 eV: CF_4, CCl_4, $CFCl_3$, CF_2Cl_2, and CF_3Cl, Communications in Theoretical Physics, 45 (2006) 697.
[39] D. Shi, J. Sun, Z. Zhu, Y. Liu, Total cross sections for electron scattering by CF_4, CCl_4, CF_2Cl_2, $CClF_3$ and $CFCl_3$ at 30–5000 eV: A modified additivity rule approach, Nuclear Instruments and Methods in Physics Research Section B: Beam Interactions with Materials and Atoms, 254 (2007) 205-210.
[40] D. Gupta, B. Antony, Total cross section for chloroflouromethanes and CCl_x radicals by electron impact, Journal of Electron Spectroscopy and Related Phenomena, 186 (2013) 25-29.

[41] H. Daimon, T. Kondow, K. Kuchitsu, Measurement of Differential Cross Sections of Low-Energy Electrons Elastically Scattered by Gas Molecules. III. Effect of Intramolecular Double Scattering as Observed in the Scattering of 70–400 eV Electrons by Carbon Tetrachloride, Journal of the Physical Society of Japan, 52 (1983) 84-89.
[42] Y. Jiang, J. Sun, L. Wan, Total cross sections for electron scattering by polyatomic molecules at 10–1000 eV: H_2S, SiH_4, CH_4, CF_4, CCl_4, SF_6, C_2H_4, CCl_3F, $CClF_3$, and CCl_2F_2, Physical Review A, 52 (1995) 398.
[43] R. Curik, F. A. Gianturco, N. Sanna, Electron and positron scattering from halogenated methanes: a comparison of elastic cross sections, Journal of Physics B: Atomic, Molecular and Optical Physics, 33 (2000) 615.
[44] P. Limão-Vieira, M. Horie, H. Kato, M. Hoshino, F. Blanco, G. García, S. J. Buckman, H. Tanaka, Differential elastic electron scattering cross sections for CCl_4 by 1.5–100 eV energy electron impact, The Journal of Chemical Physics, 135 (2011) 234309.
[45] R. F. Baker, J. T. Tate, Ionization and dissociation by electron impacf in CCl_2F_2 and in CCl_4 vapor, Phys. Rev., 53 (1938) 683.
[46] R. M. Reese, V. H. Dibeler, F. L. Mohler, Survey of negative ions in mass spectra of polyatomic molecules, J. Res. Nat. Bur. Stand, 57 (1956) 367.
[47] J. D. Craggs, C. A. McDowell, J. W. Warren, Electron capture processes in polyatomic molecules, Transactions of the Faraday Society, 48 (1952) 1093-1099.
[48] R. E. Fox, R. K. Curran, Ionization Processes in CCl_4 and SF_6 by Electron Beams, The Journal of Chemical Physics, 34 (1961) 1595-1601.
[49] S. C. Chu, P. D. Burrow, Dissociative attachment of electrons in the chloromethanes, Chemical Physics Letters, 172 (1990) 17-22.
[50] J. K. Olthoff, J. H. Moore, J. A. Tossell, Electron attachment by chloro and bromomethanes, The Journal of Chemical Physics, 85 (1986) 249-254.
[51] W. M. Hickam, D. Berg, Negative ion formation and electric breakdown in some halogenated gases, The Journal of Chemical Physics, 29 (1958) 517-523.
[52] D. Spence, G. J. Schulz, Temperature dependence of electron attachment at low energies for polyatomic molecules, The Journal of Chemical Physics, 58 (1973) 1800-1803.
[53] S. Matejcik, A. Kiendler, A. Stamatovic, T. D. Märk, A crossed beam high resolution study of dissociative electron attachment to CCl_4, International Journal of Mass Spectrometry and Ion Processes, 149 (1995) 311-319.
[54] Š. Matejčík, V. Foltin, M. Stano, J. D. Skalný, Temperature dependencies in dissociative electron attachment to CCl_4, CCl_2F_2, $CHCl_3$ and $CHBr_3$, International Journal of Mass Spectrometry, 223 (2003) 9-19.
[55] L. G. Christophorou, The dependence of the thermal electron attachment rate constant in gases and liquids on the energy position of the electron attaching state, Zeitschrift für Physikalische Chemie, 195 (1996) 195-215, and references therein.
[56] H. Shimamori, Y. Tatsumi, Y. Ogawa, T. Sunagawa, Low-energy electron attachment to molecules studied by pulse-radiolysis microwave-cavity technique combined with microwave heating, The Journal of Chemical Physics, 97 (1992) 6335-6347.
[57] J. M. Warman, M. C. Sauer, The temperature dependence of electron attachment to CCl_4, $CHCl_3$ and $C_6H_5CH_2Cl$, International Journal for Radiation Physics and Chemistry, 3 (1971) 273-282.
[58] P. Spanel, S. Matejcik, D. Smith, The varying influences of gas and electron temperatures on the rates of electron attachment to some selected molecules, Journal of Physics B: Atomic, Molecular and Optical Physics, 28 (1995) 2941.
[59] J. Fedor, O. May, M. Allan, Absolute cross sections for dissociative electron attachment to HCl, HBr, and their deuterated analogs, Physical Review A, 78 (2008) 032701.

[60] D. Klar, M.-W. Ruf, H. Hotop, Attachment of electrons to molecules at sub-millielectronvolt resolution, Chemical Physics Letters, 189 (1992) 448-454.
[61] A. Chutjian, S. H. Alajajian, S-wave threshold in electron attachment: Observations and cross sections in CCl_4 and SF_6 at ultralow electron energies, Physical Review A, 31 (1985) 2885.
[62] D. Klar, M.-W. Ruf, H. Hotop, Dissociative electron attachment to CCl_4 molecules at low electron energies with meV resolution, International Journal of Mass Spectrometry, 205 (2001) 93-110.
[63] E. Vogt, G. H. Wannier, Scattering of ions by polarization forces, Physical Review, 95 (1954) 1190.
[64] C. E. Klots, Rate constants for unimolecular decomposition at threshold, Chemical Physics Letters, 38 (1976) 61-64.
[65] M. Braun, S. Marienfeld, M. W. Ruf, H. Hotop, High-resolution electron attachment to the molecules CCl_4 and SF_6 over extended energy ranges with the (EX) LPA method, Journal of Physics B: Atomic, Molecular and Optical Physics, 42 (2009) 125202.
[66] T. G. Lee, Electron attachment coefficients of some hydrocarbon flame inhibitors, The Journal of Physical Chemistry, 67 (1963) 360-366.
[67] L. Bouby, F. Fiquet-Fayard, H. Abgrall, Compt. Rend. Acad. Sci. (Paris), 261 (1965) 4059.
[68] R. P. Blaunstein, L. G. Christophorou, Electron attachment to halogenated aliphatic hydrocarbons, The Journal of Chemical Physics, 49 (1968) 1526-1531.
[69] D. Smith, P. Ŝpanêl, Studies of Electron Attachment at Thermal Energies Using the Flowing Afterglow–Langmuir Probe Technique, Advances in Atomic, Molecular, and Optical Physics, 32 (1994) 307-343.
[70] S. J. Burns, J. M. Matthews, D. L. McFadden, Rate coefficients for dissociative electron attachment by halomethane compounds between 300 and 800 K, The Journal of Physical Chemistry, 100 (1996) 19436-19440.
[71] J. A. Ayala, W. E. Wentworth, E. C. M. Chen, Thermal electron attachment rate to carbon tetrachloride, chloroform, dichloromethane, and sulfur hexafluoride, The Journal of Physical Chemistry, 85 (1981) 3989-3994.
[72] P. D. Burrow, A. Modelli, N. S. Chiu, K. D. Jordan, Temporary negative ions in the chloromethanes $CHCl_2F$ and CCl_2F_2: Characterization of the σ* orbitals, The Journal of Chemical Physics, 77 (1982) 2699-2701.
[73] J. A. Tossell, J. W. Davenport, MS-Xα calculation of the elastic electron scattering cross sections and x-ray absorption spectra of CX_4 and SiX_4 (X= H, F, Cl), The Journal of Chemical Physics, 80 (1984) 813-821.
[74] A. Modelli, M. Guerra, D. Jones, G. Distefano, M. Tronc, Low-energy electron capture in group 14 methyl chlorides and tetrachlorides: Electron transmission and dissociative electron attachment spectra and MS-Xα calculations, The Journal of Chemical Physics, 108 (1998) 9004-9015.
[75] Z. Li, A. R. Milosavljević, I. Carmichael, S. Ptasinska, Characterization of neutral radicals from a dissociative electron attachment process, Physical Review Letters, 119 (2017) 053402.
[76] F. H. Dorman, Negative fragment ions from resonance capture processes, The Journal of Chemical Physics, 44 (1966) 3856-3863.
[77] H. U. Scheunemann, E. Illenberger, H. Baumgärtel, Dissociative electron attachment to CCl_4, $CHCl_3$, CH_2Cl_2 and CH_3Cl, Berichte der Bunsengesellschaft für Physikalische Chemie, 84 (1980) 580-585.
[78] T. Oster, A. Kühn, E. Illenberger, Gas phase negative ion chemistry, International Journal of Mass Spectrometry and Ion Processes, 89 (1989) 1-72.
[79] E. Illenberger, Energetics of Negative Ion Formation in Dissociative Electron Attachment to CCl_4, $CFCl_3$, CF_2Cl_2, and CF_3Cl, Berichte der Bunsengesellschaft für Physikalische Chemie, 86 (1982) 252-261.
[80] H. X. Wan, J. H. Moore, J. A. Tossell, Electron scattering cross sections and negative ion states of silane and halide derivatives of silane, The Journal of Chemical Physics, 91 (1989) 7340-7347.
[81] P. Możejko, G. Kasperski, C. Z. Szmytkowski, A. Zecca, G. P. Karwasz, L. Del Longo, R. S. Brusa, Absolute total cross-section measurements for electron scattering from silicon tetrachloride, SiCl,

molecules, The European Physical Journal D-Atomic, Molecular, Optical and Plasma Physics, 6 (1999) 481-485.
[82] P. Możejko, B. Żywicka-Możejko, C. Szmytkowski, Elastic cross-section calculations for electron collisions with XY_4 (X= Si, Ge; Y= H, F, Cl, Br, I) molecules, Nuclear Instruments and Methods in Physics Research Section B: Beam Interactions with Materials and Atoms, 196 (2002) 245-252.
[83] M. H. F. Bettega, Elastic collisions of low-energy electrons with SiY_4 (Y= Cl, Br, I) molecules, Physical Review A, 84 (2011) 052725.
[84] P. Verma, D. Mahato, J. Kaur, B. Antony, Electron induced inelastic and ionization cross section for plasma modeling, Physics of Plasmas, 23 (2016) 093512.
[85] R. H. Vought, Molecular Dissociation by Electron Bombardment: A Study of $SiCl_4$, Physical Review, 71 (1947) 93.
[86] B. E. Wilkerson, J. G. Dillard, Resonant electron capture in silicon tetraisocyanate and silicon tetrachloride, Journal of the Chemical Society D: Chemical Communications, (1969) 212a-212a.
[87] J. Wang, J. L. Margrave, J. L. Franklin, Interpretation of dissociative-electron attachment processes for silicon tetrachloride, Journal of Chemical Physics, 61 (1974) 1357-1360.
[88] R. E. Pabst, J. L. Margrave, J. L. Franklin, Electron impact studies of the tetrachlorides and tetrabromides of silicon and germanium, International Journal of Mass Spectrometry and Ion Physics, 25 (1977) 361-374.
[89] C. R. Moylan, S. B. Green, J. I. Brauman, Electron attachment chemistry of $SiCl_4$. Relevance to plasma reactions, International Journal of Mass Spectrometry and Ion Processes, 96 (1990) 299-307.
[90] K. Jager, A. Henglein, The Formation of Negative Ions from SiCl, and Organic Silicon Chlorides by means of Electron Impact, Z. Naturforsch. 23a, (1968) 1122-1127.
[91] C. Szmytkowski, P. Mozejko, G. Kasperski, Low-and intermediate-energy total electron scattering cross sections for SiH_4 and $GeCl_4$ molecules, Journal of Physics-London-B Atomic Molecular and Optical Physics, 30 (1997) 4363-4372.
[92] F. Guillot, C. Dézarnaud-Dandine, M. Tronc, A. Modelli, A. Lisini, P. Decleva, G. Fronzoni, Empty levels in germanium compounds studied by XAS, ISEELS, ETS, DEAS and ab initio calculations: GeH_4, $GeCl_4$ and $Ge(CH_3)_3Cl$, Chemical Physics, 205 (1996) 359-378.
[93] E. Joucoski, M. H. F. Bettega, Elastic scattering of low-energy electrons by carbon, silicon, germanium and tin tetrahalides, Journal of Physics B: Atomic, Molecular and Optical Physics, 35 (2002) 4953.
[94] B. P. Mathur, E. W. Rothe, G. P. Reck, Negative ions from reactions of alkalis with $SnCl_4$, $GeCl_4$ and $TiCl_4$, International Journal of Mass Spectrometry and Ion Physics, 31 (1979) 77-84.
[95] E. H. Bjarnason, B. Ómarsson, S. Engmann, F. H. Ómarsson, O. Ingólfsson, Dissociative electron attachment to titatinum tetrachloride and titanium tetraisopropoxide, The European Physical Journal D, 68 (2014) 121.
[96] G. J. Schulz, Cross Sections and Electron Affinity for O^- Ions From O_2, CO, and CO_2 by Electron Impact, Physical Review, 128 (1962) 178.
[97] L. G. Christophoru, Electron-Molecule Interactions and their Applications, Academic Press, Orlando, Florida, 1984.
[98] S. Matt, O. Echt, R. Wörgötter, V. Grill, P. Scheier, C. Lifshitz, T. D. Märk, Appearance and ionization energies of multiply-charged C_{70} parent ions produced by electron impact ionization, Chemical Physics Letters, 264 (1997) 149-156.
[99] B. Gstir, S. Denifl, G. Hanel, M. Rümmele, T. Fiegele, P. Cicman, M. Stano, S. Matejcik, P. Scheier, K. Becker, Electron impact multiple ionization of neon, argon and xenon atoms close to threshold: appearance energies and Wannier exponents, Journal of Physics B: Atomic, Molecular and Optical Physics, 35 (2002) 2993.

[100] P. Papp, P. Shchukin, J. Kočíšek, Š. Matejčík, Electron ionization and dissociation of aliphatic amino acids, The Journal of Chemical Physics, 137 (2012) 105101.
[101] M. Stano, S. Matejcik, J. D. Skalny, T. D. Märk, Electron impact ionization of CH_4: ionization energies and temperature effects, Journal of Physics B: Atomic, Molecular and Optical Physics, 36 (2003) 261.
[102] K. L. Nixon, W. A. D. Pires, R. F. C. Neves, H. V. Duque, D. B. Jones, M. J. Brunger, M. C. A. Lopes, Electron impact ionisation and fragmentation of methanol and ethanol, International Journal of Mass Spectrometry, 404 (2016) 48-59.
[103] F. Neese, The ORCA program system, Wiley Interdisciplinary Reviews: Computational Molecular Science, 2 (2012) 73-78.
[104] S. Grimme, Semiempirical hybrid density functional with perturbative second-order correlation, The Journal of Chemical Physics, 124 (2006) 034108.
[105] J. Noga, R. J. Bartlett, The full CCSDT model for molecular electronic structure, The Journal of Chemical Physics, 86 (1987) 7041-7050.
[106] L. Goerigk, S. Grimme, A thorough benchmark of density functional methods for general main group thermochemistry, kinetics, and noncovalent interactions, Physical Chemistry Chemical Physics, 13 (2011) 6670-6688.
[107] R. H. W. J. Ditchfield, W. J. Hehre, J. A. Pople, Self-consistent molecular-orbital methods. IX. An extended Gaussian-type basis for molecular-orbital studies of organic molecules, The Journal of Chemical Physics, 54 (1971) 724-728.
[108] T. H. Dunning Jr, Gaussian basis sets for use in correlated molecular calculations. I. The atoms boron through neon and hydrogen, The Journal of Chemical Physics, 90 (1989) 1007-1023.
[109] F. Grein, Structure and properties of the anions MF_4^-, MCl_4^- and MBr_4^-(M= C, Si, Ge), Molecular Physics, 113 (2015) 790-800.
[110] B. H. Boo, I. Koyano, Negative ion formation from photoexcited carbon tetrachloride and silicon tetrachloride studied by negative-ion mass spectrometry in the range of 12.4–31.0 eV, Journal of Electron Spectroscopy and Related Phenomena, 163 (2008) 40-44.
[111] A. Kalamarides, R. W. Marawar, M. A. Durham, B. G. Lindsay, K. A. Smith, F. B. Dunning, Use of Rydberg atoms to probe negative ion lifetimes, The Journal of Chemical Physics, 93 (1990) 4043-4046.
[112] E. P. Wigner, On the behavior of cross sections near thresholds, Physical Review, 73 (1948) 1002.
[113] A. F. Gaines, J. Kay, F. Page, Determination of electron affinities. Part 8.—Carbon tetrachloride, chloroform and hexachloroethane, Transactions of the Faraday Society, 62 (1966) 874-880.
[114] H. Dispert, K. Lacmann, Negative ion formation in collisions between potassium and fluoro-and chloromethanes: Electron affinities and bond dissociation energies, International Journal of Mass Spectrometry and Ion Physics, 28 (1978) 49-67.
[115] Y.-R. Luo, Comprehensive handbook of chemical bond energies, CRC press, Boca Raton, USA, 2007.
[116] P. C. Samartzis, I. Sakellariou, T. Gougousi, T. N. Kitsopoulos, Photofragmentation study of Cl_2 using ion imaging, The Journal of Chemical Physics, 107 (1997) 43-48.
[117] G. R. Somayajulu, Dissociation energies of diatomic molecules, The Journal of Chemical Physics, 33 (1960) 1541-1553.
[118] K. K. Murray, D. G. Leopold, T. M. Miller, W. C. Lineberger, Photoelectron spectroscopy of the halocarbene anions HCF^-, $HCCl^-$, $HCBr^-$, HCI^-, CF_2^-, and CCl_2^-, The Journal of Chemical Physics, 89 (1988) 5442-5453.
[119] U. Berzinsh, M. Gustafsson, D. Hanstorp, A. Klinkmüller, U. Ljungblad, A.-M. Mårtensson-Pendrill, Isotope shift in the electron affinity of chlorine, Physical Review A, 51 (1995) 231.
[120] W. A. Chupka, J. Berkowitz, D. Gutman, Electron affinities of halogen diatomic molecules as determined by endoergic charge transfer, The Journal of Chemical Physics, 55 (1971) 2724-2733.

[121] E. Illenberger, A method to determine excess energies in dissociative electron attachment processes, Berichte der Bunsengesellschaft für physikalische Chemie, 86 (1982) 247-252.
[122] J. Craggs, C. McDowell, The ionization and dissociation of complex molecules by electron impact, Reports on Progress in Physics, 18 (1955) 374.
[123] P. Rowntree, L. Sanche, L. Parenteau, M. Meinke, F. Weik, E. Illenberger, Dissociative electron attachment to condensed and adsorbed halomethanes, The Journal of chemical physics, 101 (1994) 4248-4259.
[124] D. Slaughter, A. Belkacem, C. McCurdy, T. Rescigno, D. Haxton, Ion-momentum imaging of dissociative attachment of electrons to molecules, Journal of Physics B: Atomic, Molecular and Optical Physics, 49 (2016) 222001.
[125] D. C. Winkler, J. H. Moore, J. A. Tossell, Inner-shell electron excitation in the chlorosilanes, Chemical Physics Letters, 219 (1994) 57-64.
[126] S. Ali, Gas phase vacuum-ultraviolet (VUV) spectroscopy of small halogenated polyatomic molecules, University of Birmingham, UK, 2007
[127] J. S. Tse, Z. F. Liu, J. D. Bozek, G. M. Bancroft, Multiple-scattering Xα study of the silicon and chlorine core-level photoabsorption spectra of $SiCl_4$, Physical Review A, 39 (1989) 1791.
[128] M. Hatano, O. Ito, Electron Donor-acceptor Complexes between Group IV Tetrahalides and Methylbenzenes, Bulletin of the Chemical Society of Japan, 44 (1971) 916-923.
[129] D. L. Hildenbrand, K. H. Lau, A. Sanjurjo, Experimental thermochemistry of the SiCl and SiBr radicals; enthalpies of formation of species in the Si−Cl and Si−Br systems, The Journal of Physical Chemistry A, 107 (2003) 5448-5451.
[130] J. Tamas, G. Czira, A. K. Maltsev, O. M. Nefedov, Electron impact studies on some organochlorogermanes: mass spectra and bond dissociation energies, Journal of Organometallic Chemistry, 40 (1972) 311-316.
[131] D. L. Hildenbrand, K. H. Lau, Dissociation energy of the molecule GeCl, Chemical Physics Letters, 263 (1996) 145-147.
[132] D. S. Slaughter, A. Belkacem, C. W. McCurdy, T. N. Rescigno, D. J. Haxton, Ion-momentum imaging of dissociative attachment of electrons to molecules, Journal of Physics B: Atomic, Molecular and Optical Physics, 49 (2016) 222001.

Tables

Table 1. Calculated threshold values (E_{th}), measured appearance energies (AEs) and energies of the intensity (Int.) maxima for the formation of negative ions from CCl_4. The AE values are determined by fitting a Wannier type function to the onset region of the individual contributions, and with a linear fit to the onset region and the rising part of the respective ion yields as described in section 2.2. The latter are reported in parenthesis. An asterisk (*) denotes values determined when only the rising part of the peak is fitted. For low intensity ion yields, the AEs are estimated from a linear fit to the rising edge of the peak above the onset region (see supporting material S1). Threshold energies are calculated at the DFT/B2PLYP and CCSD(T) level of theory. AEs and peak maxima determined in the current work are compared with that of (a) Scheunemann *et al*. [77], and peak maxima estimated from (b) Oster *et al*. [78]. All energies are in eV.

Fragments	E_{th}(CCSD)	E_{th}(B2PLYP)	AE (present)	a
CCl_3^-	0.84	0.79	0.3 ± 0.1 (0.6 ± 0.1)	0.5 ± 0.1
			5.1 ± 0.1 (5.2 ± 0.1)	—
CCl_2^-	1.71 (loss of Cl_2) 4.20 (loss of 2Cl)	1.6 (loss of Cl_2) 3.97 (loss of 2Cl)	1.2 ± 0.1 (1.3 ± 0.1)	0.9 ± 0.1
			4.8 ± 0.1 (5.1 ± 0.1)	4.7 ± 0.1
Cl_2^-	0.87	0.65	0.2 ± 0.1 (0.5 ± 0.1)	0.6 ± 0.1
			4.9 ± 0.1 (5.2 ± 0.1)	5 ± 0.2
Cl^-	-0.71	-1.03	0	0
			(0.4 ± 0.2)*	≤0.3
			(4.3 ± 0.2)*	≈4

Fragments	Peak Int. position (present)	a	b
CCl_3^-	1.3 ± 0.1	1.3 ± 0.1	≈1.2
	6.1 ± 0.1	—	—
CCl_2^-	1.8 ± 0.1	1.65 ± 0.1	≈1.7
	6.1 ± 0.1	6 ± 0.1	≈6
Cl_2^-	1.2 ± 0.1	1.1 ± 0.1	—
	6.1 ± 0.1	—	—
Cl^-	0	0	0
	0.8 ± 0.1	0.75 ± 0.05	—
	6 ± 0.1	—	—

Table 2: Relevant bond dissociation energies (BDE) of CCl_4 and electron affinities (EA) of CCl_n (n = 1-4), Cl and Cl_2 calculated at the DFT/B2PLYP and CCSD(T) level of theory. The calculated BDE and EA values are compared with selected experimentally determined literature values. All energies are in eV.

Bond	BDE(CCSD)	BDE(B2PLYP)	Experimental
CCl_3 – Cl	2.97	2.73	3.0 [113] 3.30 ± 0.3 [48] 3.0 ± 0.2 [114]
CCl_2 – Cl	2.86	2.85	2.76 ± 0.08 [derived in [115]] 3.70 ± 0.3 [114]
CCl – Cl	3.34	3.23	3.40 ± 0.13 [derived in [115]]
C – Cl	5.52	5.93	3.90 ± 0.13 [derived in [115]] 3.17 ± 0.1 [78]
Cl – Cl	2.49	2.37	2.40 ± 0.02 [116] 2.39 ± 0.02 [117]
Species	EA(CCSD)	EA(B2PLYP)	Experimental
CCl_4	0.77	0.87	0.94 [72]
CCl_3	2.13	1.94	2.5 ± 0.2 [79] 1.3 ± 0.3 [114]
CCl_2	1.63	1.60	1.60 [118] 1.8 ± 0.3 [114]
CCl	0.04	-0.14	—
Cl	3.68	3.76	3.61 [119]
Cl_2	2.47	2.55	2.9 ± 0.3 [79] 2.38 ± 0.1 [120]

Table 3. Calculated threshold values (E_{th}), measured appearance energies (AE) and the energies of the peak intensity maxima for the formation of negative ions from $SiCl_4$. The AE values are determined by fitting a Wannier type function to the onset region of the individual contributions, and with a linear fit to the onset region and the rising part of the respective ion yields as described in section 2.2. The latter are reported in parenthesis. An asterisk (*) denotes values determined when only the rising part of the peak is fitted. Threshold energies are calculated at the B2PLYP and CCSD(T) level of theory. AEs determined in the current work are compared with those from (a) Jäger *et al*. [90] and (b) Wang *et al* [87]. Peak maxima are compared with (a) Jäger *et al*. [90] and (b) Wang *et al* [87], (c) Pabst *et al*. [88]. and (d) Moylan *et al*. [89]. All energies are in eV.

Fragments	E_{th}(CCSD)	E_{th}(B2PLYP)	AE (present)	a	b
$SiCl_4^-$	-0.14	-0.4	0	0	0
$SiCl_3^-$	1.74	1.7	1.6 ± 0.2 (1.6 ± 0.1)	1.7	—
			5.8 ± 0.3 (6.1 ± 0.2)	5.9	—
$SiCl_2^-$	3.94	3.78	6.7 ± 0.1 (6.8 ± 0.1)	6.7	—
Cl_2^-	2.73	2.4	6.2 ± 0.1 (6.2 ± 0.1)	6.5	—
Cl^-	1.13	0.77	(1.2 ± 0.2)*	1.4	1.2
			5.9 ± 0.1 (6.1 ± 0.1)	6.1	6.8
Fragments	Peak Int. position (present)	a	b	c	d
$SiCl_4^-$	0	≈0.3	0.5	—	≈2
$SiCl_3^-$	2.1 ± 0.1	≈2.0	—	—	—
	6.9 ± 0.1	≈6.6	—	≈7.1	≈8.2
$SiCl_2^-$	7.7 ± 0.1	—	—	≈8.6	—
Cl_2^-	7.7 ± 0.1	—	—	≈8.8	—
Cl^-	1.8 ± 0.1	≈1.8	1.8	≈1.6	≈2
	7.1 ± 0.1	≈6.9	7.8	≈7.5	≈10.5

Table 4. Relevant bond dissociation energy (BDE) of $SiCl_4$ and electron affinities (EA) of $SiCl_n$ (n = 1-4), as calculated at the B2PLYP and CCSD(T) level of theory. The calculated BDE and EA values are compared with experimentally determined literature values. Note that the literature value for $SiCl_4$ is the vertical EA. All energies are in eV.

Bond	BDE(CCSD)	BDE(B2PLYP)	Experimental
$SiCl_3$ – Cl	4.81	4.54	4.66 ± 0.04 [129]
$SiCl_2$ – Cl	2.87	2.79	2.8 ± 0.04 [derived in [115]]
SiCl – Cl	4.53	4.38	4.35 ± 0.06 [derived in [115]]
Si – Cl	5.26	5.47	4.17 ± 0.06 [derived in [115]]
Species	EA(CCSD)	EA(B2PLYP)	Experimental
$SiCl_4$	0.14	0.40	-0.3 (vertical) [128]
$SiCl_3$	2.99	2.84	1.1 [88]
$SiCl_2$	1.25	1.16	≥2.6 [85] 0.9 [88]
SiCl	0.51	0.30	—

Table 5. Calculated threshold values (E_{th}), measured appearance energies (AE) and the energies of peak intensity maxima for the formation of negative ions from $GeCl_4$. The AE values are determined by fitting a Wannier type function to the onset region of the individual contributions, and with a linear fit to the onset region and the rising side of the respective ion yields as described in section 2.2. The latter are reported in parenthesis. An asterisk (*) denotes values determined when only the rising part of the peak is fitted. Threshold energies are calculated at the B2PLYP and CCSD(T) level of theory. Appearance energies determined in the current work are compared with those reported by (a) Guillot *et al.* [92], the peak maxima energies are additionally compared with those shown by, (b) Modelli *et al.* [74] and (c) Pabst *et al.* [88]. All energies are in eV.

Fragments	E_{th}(CCSD)	E_{th}(B2PLYP)	AE (present)	a
$GeCl_3^-$	0.31	0.09	0	0
			(0.8 ± 0.2)*	—
			3.1 ± 0.2	
			(3.2 ± 0.1)	—
$GeCl_2^-$	2.32	1.98	4.2 ± 0.1 (4.5 ± 0.1)	4.6 ± 0.3
Cl_2^-	1.34	0.85	(0.8 ± 0.2)*	—
			3.9 ± 0.1 (4.4 ± 0.1)	—
Cl^-	0.46	0.02	3.3 ± 0.2 (4.0 ± 0.1)	4 ± 0.3
Fragments	Peak Int. position (present)	a	b	c
$GeCl_3^-$	0	0	0	—
	1.3 ± 0.1	—	—	≈2
	5.0 ± 0.1	—	—	≈5
$GeCl_2^-$	5.8 ± 0.1	≈5.7	≈5.7	≈6.1
Cl_2^-	1.4 ± 0.1	—	—	—
	6.0 ± 0.1	—	—	≈5.7
Cl^-	5.5 ± 0.1	≈5.5	≈5.5	≈5.1

Table 6. Relevant bond dissociation energies (BDEs) for sequential Cl loss from $GeCl_4$ and electron affinities (EA) of $GeCl_n$ (n = 1-4), as calculated at the B2PLYP and CCSD(T) level of theory. Calculated BDE and EA values are compared with experimentally determined values, where available. Note, that for intact $GeCl_4$ this is the vertical EA. All energies are in eV.

Bond	BDE(CCSD)	BDE(B2PLYP)	Experimental
$GeCl_3$ – Cl	4.14	3.78	3.5 ± 0.5 [derived in [115]] 3.1 ± 0.2 [130] 3 [94]
$GeCl_2$ – Cl	2.16	1.99	2.2 ± 0.5 [derived in [115]
GeCl – Cl	4.29	4.10	3.6 ± 0.2 [derived in [115]] 3.9 [131]
Ge – Cl	5.08	5.15	3.9 ± 0.1 [131] 4.2± 0.2 [derived in [115]]
Species	EA(CCSD)	EA(B2PLYP)	Experimental
$GeCl_4$	1.54	1.80	0.87 (vertical) [128]
$GeCl_3$	3.83	3.70	1.8± 0.1 [88] >2.61 [94]
$GeCl_2$	1.49	1.42	0.31 [88]
GeCl	0.62	0.43	—